

2010

# The role of mammalian WDR1 and its truncated isoform in cell migration and cofilin signalling

Jessica Cucullo  
*University of Windsor*

Follow this and additional works at: <https://scholar.uwindsor.ca/etd>

---

## Recommended Citation

Cucullo, Jessica, "The role of mammalian WDR1 and its truncated isoform in cell migration and cofilin signalling" (2010). *Electronic Theses and Dissertations*. 281.  
<https://scholar.uwindsor.ca/etd/281>

This online database contains the full-text of PhD dissertations and Masters' theses of University of Windsor students from 1954 forward. These documents are made available for personal study and research purposes only, in accordance with the Canadian Copyright Act and the Creative Commons license—CC BY-NC-ND (Attribution, Non-Commercial, No Derivative Works). Under this license, works must always be attributed to the copyright holder (original author), cannot be used for any commercial purposes, and may not be altered. Any other use would require the permission of the copyright holder. Students may inquire about withdrawing their dissertation and/or thesis from this database. For additional inquiries, please contact the repository administrator via email ([scholarship@uwindsor.ca](mailto:scholarship@uwindsor.ca)) or by telephone at 519-253-3000ext. 3208.

THE ROLE OF MAMMALIAN WDR1 AND ITS TRUNCATED ISOFORM IN CELL  
MIGRATION AND COFILIN SIGNALLING

by  
Jessica Cucullo

A Thesis  
Submitted to the Faculty of Graduate Studies  
through Biological Sciences  
in Partial Fulfillment of the Requirements for  
the Degree of Master of Science at the  
University of Windsor

Windsor, Ontario, Canada

2009

© 2009 Jessica Cucullo

THE ROLE OF MAMMALIAN WDR1 AND ITS TRUNCATED ISOFORM IN CELL  
MIGRATION AND COFILIN SIGNALLING

by  
Jessica Cucullo

APPROVED BY:

---

Dr. S. Ananvoranich  
Department of Chemistry and Biochemistry

---

Dr. J. Hudson  
Department of Biological Sciences

---

Dr. A. Hubberstey, Advisor  
Department of Biological Sciences

---

Dr. D. Higgs, Chair of Defense  
Department of Biological Sciences

4 December 2009

## **Author's Declaration of Originality**

I hereby certify that I am the sole author of this thesis and that no part of this thesis has been published or submitted for publication.

I certify that, to the best of my knowledge, my thesis does not infringe upon anyone's copyright nor violate any proprietary rights and that any ideas, techniques, quotations, or any other material from the work of other people included in my thesis, published or otherwise, are fully acknowledged in accordance with the standard referencing practices. Furthermore, to the extent that I have included copyrighted material that surpasses the bounds of fair dealing within the meaning of the Canada Copyright Act, I certify that I have obtained a written permission from the copyright owner(s) to include such material(s) in my thesis and have included copies of such copyright clearances to my appendix.

I declare that this is a true copy of my thesis, including any final revisions, as approved by my thesis committee and the Graduate Studies office, and that this thesis has not been submitted for a higher degree to any other University or Institution.

## **Abstract**

Directed cellular migration is a normal process which involves the actin cytoskeleton and actin-binding proteins such as WDR1 and cofilin. WDR1 promotes actin filament depolymerization by enhancing the severing activity of cofilin, as well as by capping barbed ends. My research focuses on understanding the involvement of mammalian WDR1 and its truncated isoform, WDR $\Delta$ 35, in cellular migration and invasion. It also focuses on understanding the relationship between the WDR1 isoforms and cofilin activation. This study found that WDR1 and WDR $\Delta$ 35 may play a role during cancer cell motility. Also, it was revealed that cofilin enhances the transcriptional expression of WDR $\Delta$ 35. Epidermal growth factor (EGF) stimulation influenced WDR $\Delta$ 35 to increase total cofilin expression and activation, and caused WDR1 to stabilize the inactivation/phosphorylation of cofilin. In general, WDR1 and WDR $\Delta$ 35 may be functionally distinct, as their effects on motility, regulation, and cofilin activation were notably different.

## **Acknowledgments**

I would like to thank my supervisor, Dr. Andrew Hubberstey, for his expertise, and for the opportunity to undertake this research. I would like to thank my committee members, Dr. Sirinart Ananvoranich and Dr. John Hudson, for their ideas and encouragement throughout. I would like to thank past and present members of the Hubberstey lab, Rohann Correa for being a wonderful colleague and teacher, and Katie Faccechia, Milica Kovacevich, Mihaela Pupavac, Renee Tousignant, Hanna Vasilevski, and Rebecca Williams for their knowledge. I would especially like to thank former members Ryan Ard and Beth Yaworsky for their assistance, support, uplifting sarcasm, unrelenting humour, and continued friendship. Additionally, I would like to acknowledge Dr. Lisa Porter, and the Porter, Hudson, and Swan labs for their advice, guidance, and willingness to help. I would further like to extend a thank you to all faculty members, staff and fellow graduate students in the department for their assistance and guidance, especially those with whom I was fortunate enough to work directly. I would like to acknowledge the faculties of Science, Biology, and Chemistry and Biochemistry.

Finally, I have an immense amount of gratitude and appreciation for my family, John, Ruth, and Chris Cucullo, for their encouragement, unconditional support, laughter, and patience, and for my fiancé Rick Miller, for his constant understanding, optimism, and endless support and love. Thank you for all of your sacrifices. Thank you for keeping me on track when situations were not ideal and when daunting challenges arose, and for putting things into perspective.

## Table of Contents

Author's Declaration of Originality.....	iii
Abstract.....	iv
Acknowledgements.....	v
List of Figures.....	ix
List of Abbreviations.....	xi
<b>Chapter One: Introduction.....</b>	<b>1</b>
Actin.....	2
Actin-Binding Proteins.....	3
Cofilin.....	3
Aip1.....	5
WDR1.....	7
WDR $\Delta$ 35.....	8
Actin-Based Cell Migration.....	9
The Role of Cofilin during Cell Migration.....	12
The Role of Aip1/WDR1 during Cell Migration.....	15
Cancer and Metastasis.....	17
Actin-based Cell Motility in Cancer.....	18
Summary.....	21
<b>Chapter Two: Materials and Methods.....</b>	<b>22</b>
Cell Culture.....	22

DNA Extraction.....	22
DNA Transfection.....	23
Stable Cell Line Selection.....	24
X-gal Staining of Mammalian Cells.....	25
Protein Extraction.....	25
Immunoblotting.....	26
Immunofluorescence.....	27
EGF Timecourse.....	27
RNA Extraction.....	28
RT-PCR.....	28
Quantitative Real Time-PCR.....	28
Wound Healing Assay.....	29
Invasion Assay.....	30
<b>Chapter Three: Results</b> .....	<b>31</b>
Stable MCF7 cell line generation to express WDR1 proteins.....	31
GFP-fusion proteins are transiently expressed and maintained in MCF7 and Hs578T cells.....	33
WDR1 or WDR $\Delta$ 35 overexpression does not affect migration rate or invasiveness.....	37
A regulatory relationship exists between WDR1, WDR $\Delta$ 35, and cofilin in Hek293 cells.....	48
WDR $\Delta$ 35 and cofilin may transcriptionally regulate each other in MCF7 cells.....	51
Cofilin upregulates WDR $\Delta$ 35 and WDR1 downregulates WDR $\Delta$ 35 in Hs578T cells.....	53



WDR1 and WDR $\Delta$ 35 transcription is not affected by brief activation of the EGF-cofilin pathway.....	53
In MCF7 cells, WDR1 protein expression stabilizes inactivation of cofilin, while WDR $\Delta$ 35 expression increases total cofilin.....	55
In Hs578T cells, WDR1 protein expression stabilizes inactivation of cofilin, while WDR $\Delta$ 35 increases total cofilin.....	59
<b>Chapter Four: Discussion</b> .....	64
<b>Chapter Five: Conclusions</b> .....	72
<b>References</b> .....	74
<b>Appendix A</b> .....	85
<b>Vita Auctoris</b> .....	86

## List of Figures

Figure 1.1: The process of actin-based cellular migration.....	11
Figure 1.2: The cofilin regulation pathway.....	14
Figure 3.1: Stable GFP fusion proteins can be inducibly expressed in Hek293 cells.....	32
Figure 3.2: Only one stable MCF7 cell line, GFP-4, was successfully created.....	34
Figure 3.3: No stable HA MCF7 cell lines were successfully created.....	36
Figure 3.4: GFP-tagged WDR1 and WDR $\Delta$ 35 maintained consistent levels of transient expression for up to 72hr.....	38
Figure 3.5: GFP-WDR1 and GFP-WDR $\Delta$ 35 are expressed in MCF7 and Hs578T cells after transient transfection.....	39
Figure 3.6: Transient overexpression of WDR1 or WDR $\Delta$ 35 does not significantly affect migration rate of MCF7 or Hs578T cells.....	43
Figure 3.7: Transient overexpression of WDR1 or WDR $\Delta$ 35 does not significantly affect MCF7 or Hs578T invasiveness.....	47
Figure 3.8: In stable Hek293 cells, cofilin upregulates WDR $\Delta$ 35 and WDR $\Delta$ 35 downregulates WDR1 at the transcriptional level.....	49
Figure 3.9: In stable TREX cells, the affects of GFP-WDR1 or GFP-WDR $\Delta$ 35 on cofilin translation are negligible.....	50
Figure 3.10: In MCF7 cells, WDR1 and WDR $\Delta$ 35 downregulate cofilin, and cofilin upregulates WDR $\Delta$ 35.....	52
Figure 3.11: In Hs578T cells, cofilin and WDR1 expression have opposite effects on WDR $\Delta$ 35 transcription levels.....	54

Figure 3.12: During induction of the cofilin regulation pathway in MCF7 cells, GFP-WDR1 stabilizes inactive cofilin, while GFP-WDR $\Delta$ 35 increases active cofilin.....	56
Figure 3.13: During induction of the cofilin regulation pathway in Hs578T cells, GFP-WDR1 stabilizes inactive cofilin, while GFP-WDR $\Delta$ 35 increases active cofilin.....	60
Figure 4.1: Human WDR1 and WDR $\Delta$ 35 protein sequence alignment and proposed functional residues.....	65

## List of Abbreviations

- ABP – actin binding protein
- ADF – actin depolymerizing factor
- Aip1 – actin interacting protein 1
- Arp2/3 – actin related protein 2/3
- BSA – bovine serum albumin
- CC – critical concentration
- CMV - cytomegalovirus
- CS - coverslip
- DAG - diacylglycerol
- DMEM – Dulbecco`s modified Eagle`s medium
- Dox or (+) - doxycycline
- ECM – extracellular matrix
- EDTA – Ethylenediaminetetraacetic acid
- EGF – epidermal growth factor
- FBS – fetal bovine serum
- GAPDH - glyceraldehyde-3-phosphate dehydrogenase
- GFP – green fluorescent protein
- HA - hemagglutinin
- Hek293 – human embryonic kidney 293 cell line
- HRP – horseradish peroxidase
- IP<sub>3</sub> - inositol 1,4,5-triphosphate
- LB – Luria Bertani

LIMK – LIM-kinase

logRQ – log of the relative quantification value

MMP – matrix metalloproteinases

OD – optical density

PEI - polyethylenimine

PI3K - phosphoinositide-3-kinase

PIP<sub>2</sub> - phosphatidylinositol 4,5-bisphosphate

PLC - phospholipase C

RIPA – radioimmunoprecipitation assay

ROCK - Rho-associated coil-coil-forming kinase

SFM – serum-free medium

SSH - slingshot

TAM – tumour-associated macrophages

TBST – Tris-buffered saline with Tween 20

TREX – reverse tetracycline transactivator-expressing Hek293 cells

WASP – Wiskott-Aldrich syndrome protein

WD – tryptophan-aspartic acid

WDR1 - tryptophan-aspartic acid repeat protein 1

X-gal – X-galactose

## Chapter One: Introduction

The cytoskeleton is a dynamic structure that is involved in many essential processes including cell division, vesicle transport, neurogenesis, and cell migration. There are three major components of the cytoskeleton: intermediate filaments, microtubules, and microfilaments. Various types of intermediate filaments exist, such as keratin and vimentin, and generally possess a structural role within the cell. Microtubules are comprised of  $\alpha$ - and  $\beta$ -tubulin subunits, and have both dynamic structural and regulatory roles. Microfilaments consist of polymerized actin subunits, and have active roles pertaining to the structure and regulation of the cell. Each component of the cytoskeleton has distinct and separate functions, yet cooperates as a whole system (Alberts *et al.*, 2008).

In order to carry out cellular processes properly, the actin cytoskeleton must undergo rapid actin turnover (Wegner, 1976). Alone, the actin filaments are not recycled efficiently. Consequently, actin binding proteins (ABPs) are a necessity for proper actin dynamics. This includes proteins for actin nucleation, depolymerization, polymerization, and severing. One of these proteins, cofilin, acts to sever and depolymerize the filaments (Bamburg *et al.*, 1980; Dos Remedios *et al.*, 2003). Another is Aip1, or actin-interacting protein-1, which enhances cofilin activity (Rodal *et al.*, 1999; Ono, 2003). Regulation of actin turnover leads to the formation of membrane protrusions, allowing for cell migration to occur (Svitkina and Borisy, 1999). Furthermore, the actin cytoskeleton and many of its associated proteins are necessary during migration and invasion of cancer

cells (Condeelis *et al.*, 2005). The purpose of this study is to explore the function of mammalian Aip1 and its relationship with cofilin.

## **Actin**

Actin is a 42kDa protein, which is highly conserved in all eukaryotes. In humans, six genes encode different forms of actin, which are specific to certain tissues. Generally, actin is found in two forms, globular or G-actin, and filamentous or F-actin. G-actin is bound to ATP, while F-actin is ADP-bound. Relatively flexible microfilaments are formed when G-actin, or monomeric actin, polymerizes into F-actin strands with the concomitant hydrolysis of ATP to ADP. These strands are wound together in a helix formation. Microfilaments have a diameter of 7nm and each turn in the helix occurs every 37nm. Microfilaments are polarized, meaning that they possess a pointed, or minus end and a barbed, or plus end. If actin monomer concentration within the cytosol is above a critical concentration (CC), filament elongation can occur. Polymerization is favoured at the barbed end, while depolymerization of the filament into actin monomers is favoured at the pointed end (Hill and Kirschner, 1982). A process called treadmilling occurs along the filament if actin subunit concentration is higher than the barbed-end CC and lower than the pointed-end CC. This means that polymerization and depolymerization rates are equivalent. Treadmilling results in actin turnover, which is an essential aspect of cell migration and other cellular events (Wegner, 1976; Wang, 1985). For this process to be efficient, it must be aided by a number of ABPs (Dos Remedios *et al.*, 2003).

## **Actin-Binding Proteins**

The actin cytoskeleton is regulated by several categories of associated proteins. Without these proteins, cytoskeletal processes would be highly inefficient. Proteins such as actin-related protein-2/3 (Arp2/3) act as actin filament nucleators. Arp2/3 allows for new filaments to form and creates branched actin networks within the cell (Welch *et al.*, 1997; Dos Remedios *et al.*, 2003). Actin-sequestering proteins such as profilin bind to actin monomers. Through binding, profilin promotes exchange of ADP to ATP, thus allowing addition of the actin monomer to the barbed end (Goldschmidt-Clermont *et al.*, 1991; Dos Remedios *et al.*, 2003). In contrast, other proteins aid in the severing and depolymerization of actin filaments. One such protein, cofilin, severs filaments and also promotes depolymerization, thus it largely contributes to treadmilling. Once severing occurs, cofilin can bind to ADP-bound actin to inhibit nucleotide exchange once disassembly occurs, and thus its availability for polymerization at the barbed end is limited (Carlier *et al.*, 1997; Dos Remedios *et al.*, 2003). Depolymerization is also promoted when other ABPs, known as filament capping proteins, are recruited by cofilin (Dos Remedios *et al.*, 2003). Capping proteins such as CapZ and Aip1 bind to barbed ends and prevent addition of actin monomers to the filament, thus enhancing cofilin's depolymerizing function (Sept *et al.*, 1999; Dos Remedios *et al.*, 2003; Ono, 2003).

### **Cofilin**

Cofilin is an ABP that was originally discovered in chicken and porcine brain tissue (Bamburg *et al.*, 1980; Nishida *et al.*, 1984). In mammals, the actin-depolymerizing factor (ADF)/cofilin family consists of three isoforms: cofilin-1, cofilin-2, and ADF. Cofilin-1, or nonmuscle cofilin, is the dominant isoform and is ubiquitously expressed in



most cell types (Ono *et al.*, 2004). Cofilin-2, or muscle cofilin, is the dominant isoform expressed in cardiac muscle cells and the only one expressed in differentiated skeletal muscle cells. ADF, also called destrin, tends to show higher levels of expression in epithelial and endothelial tissues (Ono *et al.*, 1994; Nakashima *et al.*, 2005; van Troys *et al.*, 2008). Although these different isoforms exhibit varied expression, structurally, they are highly conserved. Each one is constituted by a single-fold domain called an ADF-homology domain, which is also known to be present in other ABP families. (Lappalainen *et al.*, 1998; Maciver and Hussey, 2003; van Troys *et al.*, 2008). Although cofilin itself is conserved, the number and type of isoforms that exist in different organisms vary. In *Caenorhabditis elegans*, the ADF/cofilin gene *unc-60* encodes both UNC-60A and UNC-60B proteins (Ono and Benian, 1998). In *Arabidopsis thaliana*, there are twelve separate ADF/cofilin genes (Dong *et al.*, 2001). In contrast, the *Saccharomyces cerevisiae* genome contains only one ADF/cofilin gene (Iida *et al.*, 1993; Moon *et al.*, 1993).

Cofilin-1 is a relatively small protein of 19kDa, but plays a significant role in actin dynamics. This protein has two major functions that both contribute to actin turnover: severing and depolymerizing of F-actin (Carlier *et al.*, 1997; Bamburg and Wiggins, 2002; van Troys *et al.*, 2008). In recent years, it has been shown that the concentration of cofilin within the cell dictates its activity. At low concentrations, cofilin tends to sever filaments, whereas increased polymerizing activity is observed at higher levels (Andrianantoandro and Pollard, 2006; van Troys *et al.*, 2008). Severing occurs when cofilin binds to F-actin, causing a conformational change, or twisting of the filament. The effect of this change is thought to extend hundreds of actin subunits along

the filament, forcing the structure to fracture. Cofilin's severing action ultimately generates newly-available barbed ends (van Troys *et al.*, 2008). As a depolymerizing protein, cofilin increases the off-rate of ADP-actin at the pointed end by 30-fold. This occurs since cofilin has a higher affinity for ADP-actin than ATP-actin, and once bound it causes a slight angular rotation of the monomers (Carlier *et al.*, 1997; van Troys *et al.*, 2008). Furthermore, evidence has also shown that Aip1 can enhance cofilin's function by capping barbed ends of filaments, thus temporarily inhibiting polymerization and reassociation of severed ends (Okada *et al.*, 2002; Balcer *et al.*, 2003). Actin filament disassembly via filament-bound cofilin is activated by the N-terminal propeller of Aip1 (Rodal *et al.*, 1999; Li *et al.*, 2007). Ultimately, these cofilin-Aip1-mediated activities lead to a net polymerization, since new filaments can grow from severed ones and depolymerized actin is recycled (Clark *et al.*, 2006).

### **Aip1**

Aip1 was originally discovered in yeast (Amberg *et al.*, 1995). Since then, homologs in several other species such as *C. elegans*, *Dictyostelium discoideum*, *Xenopus laevis*, *Drosophila melanogaster*, and *Homo sapiens* have been studied. Aip1 is a 67kDa protein and is part of the tryptophan-aspartic acid (WD) repeat family of proteins (Ono, 2001; Voegtli *et al.*, 2003). WD40 repeat sequences consist of approximately 40 amino acids that form one blade of one overall  $\beta$ -propeller structure. The domains formed by these repeats are commonly involved in regulation and reversible binding of target proteins (Smith *et al.*, 1999). Aip1 is unique in terms of  $\beta$ -propeller proteins because it has two propeller domains each made up of 7 blades (Voegtli *et al.*, 2003; Mohri *et al.*,

2004). This distinctive configuration of Aip1 has been described as a clam-shell formation, since the two propeller domains are set at a 110° angle. (Voegtli *et al.*, 2003).

As previously mentioned, Aip1 is an ABP that can associate with both actin and cofilin to regulate cofilin-mediated actin filament dynamics (Mohri *et al.*, 2004). Aip1 has two separate functions: to enhance cofilin's ability to sever and disassemble actin filaments and to cap barbed ends of cofilin-bound filaments (Rodal *et al.*, 1999; Okada *et al.*, 2002; Balcer *et al.*, 2003; Mohri *et al.*, 2006; Li *et al.*, 2007; Tsuji *et al.*, 2009). A series of studies examining the functional relationship between *C. elegans* Aip1/UNC-78 and cofilin/UNC-60 determined that four conserved Aip1/UNC-78 residues, E126, D168, F182, and F192, are responsible for binding to cofilin/UNC-60-bound actin and activating disassembly of filaments. These residues are found on the external area of blades 3 and 4 of the N-terminal  $\beta$ -propeller domain. To further characterize this interaction, it was shown that individual point mutations at these residues generally did not affect Aip1/UNC-78 function. However, a quadruple mutation of these residues eliminated its actin disassembly function altogether. In addition, another residue, G19, was shown to be crucial for Aip1/UNC-78's barbed-end capping ability. All aspects of these studies imply that Aip1 is necessary to augment cofilin's function (Mohri *et al.*, 2004; Mohri *et al.*, 2006). These findings coincide with other studies concluding that conversely, the presence of cofilin induces filament disassembly by Aip1, and that Aip1 alone has minimal influence on these dynamics (Mohri and Ono, 2003; Ono, 2003).

Aip1 is a well conserved protein that has also been studied using other model systems. A *Dictyostelium* homolog, DAip1, was discovered by Konzok *et al.* (1999). It was suggested to play a contributing role in regulating filament disassembly alongside

cofilin, although mutations did not severely affect its function. In contrast, vertebrate homologs of Aip1 such as XAip1 in *Xenopus*, exhibit strong correlations with cofilin-mediated actin disassembly. XAip1 localizes with cofilin, with higher concentrations in cortical regions. XAip1's association with cofilin-bound actin enables its barbed-end capping function, which in turn assists cofilin's depolymerizing and severing effects (Okada *et al.*, 1999; Kueh *et al.*, 2008). In a study on *Xenopus* blastomeres, increased amounts of shortened actin filaments were detected in the presence of cofilin and XAip1 together compared to filaments subjected to cofilin or XAip1 alone (Okada *et al.*, 1999).

### **WDR1**

WD40 Repeat protein 1 (WDR1) is the ~67kDa vertebrate homolog of yeast Aip1 and was first noted in chickens by Adler *et al.* (1999). WDR1 contains nine WD repeats of 30-40 amino acids, each of which comprises a single blade of the  $\beta$ -propeller domain structure (Adler *et al.*, 1999; Smith *et al.*, 1999; Voegtli *et al.*, 2003). Six kelch-like motifs have also been identified in human and rat WDR1 and are adjacent to the WD motifs (Noone and Hubberstey, unpublished). Kelch motifs are generally 44-56 amino acids in length, repeat in groups of 5-7, and much like WD repeats, each form a blade as part of a  $\beta$ -propeller structure. Many kelch proteins bind F-actin and may have specific binding partners (Prag and Adams, 2003). In the case of WDR1, its binding partner would be cofilin, further suggesting it is a kelch-like protein.

WDR1 has been actively studied. Overall, when compared to Aip1, WDR1 exhibits similar roles in cofilin-mediated actin dynamics. In rat pheochromocytoma cells, WDR1 co-localizes with actin (Shin *et al.*, 2004). In mouse megakaryocytes and neutrophils, mutating WDR1 causes macrothrombocytopenia and autoinflammatory

disease due to impaired cofilin-mediated actin processes (Kile *et al.*, 2007). Other studies have indicated that WDR1 may have additional roles within the cell. Expression was upregulated after chicks were subjected to noise trauma, indicating that a stress response function through increased actin turnover is a possibility for WDR1 (Adler *et al.*, 1999; Adler *et al.*, 2008).

Additionally, a study by Noone and Hubberstey (unpublished) has investigated the function, localization, and expression of a 60kDa WDR1 in rats and humans. In rat fibroblast cells, WDR1 localizes to the ends of actin filaments and is distributed along the filaments themselves. These findings are consistent with actin disassembly and capping functions. Direct actin-WDR1 interactions were also observed. Furthermore, human WDR1 is not expressed in heart or skeletal muscle tissue. Generally, many aspects of WDR1 are still unclear, including its interaction with cofilin, effect on cytoskeletal processes like migration, and more specific expression levels and patterns. In addition, more mutational analyses of WDR1 would shed light on any functions that are specific to higher eukaryotes.

### **WDR $\Delta$ 35**

Recently, a truncated isoform of human WDR1 named WDR $\Delta$ 35 was discovered. Exons three, four, and five (421-840bp) are excised from this isoform, yielding a protein of ~42kDa. While all six kelch-like regions are preserved in WDR $\Delta$ 35, splicing removes three of the nine WD repeats (Noone and Hubberstey, unpublished). More information is required to determine if WDR1 and WDR $\Delta$ 35 arise from different transcriptional start sites or through alternative splicing. It is not known if this second isoform is also expressed in other organisms besides mammals, as it has only been studied in humans and

rats. Interestingly, WDR $\Delta$ 35 is expressed in heart and skeletal muscle tissue, the same two tissues that lack expression of WDR1 (Noone and Hubberstey, unpublished). Cofilin-2 (muscle cofilin) is also the only isoform expressed in skeletal muscle, and is expressed dominantly in cardiac muscle (Ono *et al.*, 1994; Nakashima *et al.*, 2005). Thus, specific expression of cofilin and WDR1 isoforms in these tissues may allude to the function of WDR $\Delta$ 35. Additionally, WDR $\Delta$ 35 expression is significantly higher than WDR1 expression in other human tissues and cell lines (Correa and Hubberstey, unpublished data). Although its function is entirely unknown, these data suggest the possibility that WDR $\Delta$ 35 may be the dominant mammalian isoform or that its role within the cell differs from WDR1.

### **Actin-Based Cell Migration**

Cell migration is necessary for such processes as wound-healing, development, and immune response. In order for directed cell migration to occur, the cell must first become polarized. Polarization is instigated when cells receive extracellular stimulation from chemoattractant gradients via membrane receptors. Cells that migrate by crawling do so in four general steps: protrusion, adhesion, translocation, and retraction (Figure 1.1). The actin cytoskeleton plays a major role during each step (Yamazaki *et al.*, 2005). Membrane protrusions such as lamellipodia, filopodia, podosomes, and invadopodia form at the leading edge of migratory cells. Formation of all protrusions relies on rapid actin turnover signalled by extracellular stimulants. Lamellipodia are flat, sheet-like structures and are the most common protrusion. They contain dense actin networks, which are regulated by the Arp2/3 complex (Machesky *et al.*, 1997). Signal transduction from extracellular growth factors via G-protein coupled receptors to Arp2/3's effector,

Wiskott-Aldrich syndrome protein (WASP), enables nucleation and elongation of new actin filaments. These new filaments are nucleated alongside an established filament, and polymerize at a 70° angle to form branched actin networks (Goley and Welch, 2006). Filopodia are long spindle-like projections at the cell front that act to integrate extracellular stimulants such as growth factors and nutrients. With regard to the cytoskeleton, filopodia contain long bundles of actin filaments. Their formation relies on actin polymerization being unimpeded by capping proteins at certain points along the leading edge (Lundquist, 2009). Podosomes are typically found in monocytes and osteoclasts (Linder and Kopp, 2005), while invadopodia are exclusive to cancer cells. Both of these protrusion types have a rich actin core regulated by Arp2/3, which is encompassed by integrins and integrin-related proteins (Lundquist, 2009). They also have extracellular matrix-degrading capabilities and their formation may be coupled between independent cells via paracrine signalling (Yamaguchi *et al.*, 2006).

During migration, adhesion structures such as focal complexes, focal adhesions, and fibrillar adhesions, form at the leading edge and disengage at the cell's trailing end. These structures are linked to the actin cytoskeleton by integrins. Stress fibres consist of actin and myosin bundles and work synergistically with focal adhesions. Adhesions promote stress fibre formation, and are sustained by mechanical tension created by those same fibres (Le Clairche and Carlier, 2008). Regulatory proteins that control Arp2/3

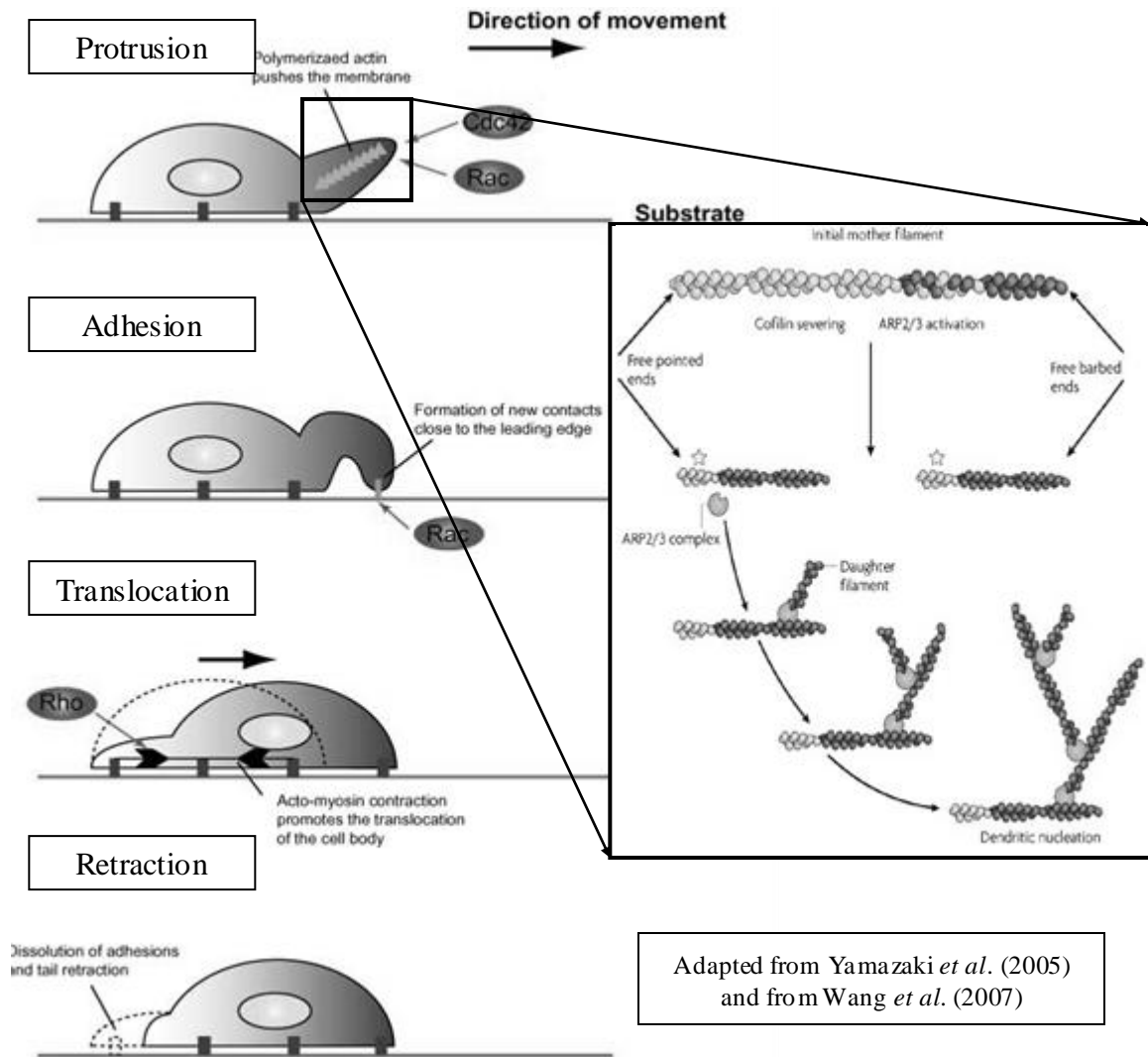


**Figure 1.1: The process of actin-based cellular migration.** Protrusion initiates when chemotactic factors induce signal transduction pathways involving Rac and Cdc42. Downstream ABPs like cofilin and Arp2/3 promote actin polymerization and branching at the leading edge (inset). Adhesion relies on integrins to mediate cell-to-matrix contact. Within the cell, integrins are linked to actin networks. During translocation, the cell body shifts forward via the actomyosin complex. Retraction involves disassembly of any previously formed adhesions at the trailing edge. Together, these steps allow the cell to detach and reattach in a coordinated and directed fashion.



activity are also responsible for the formation of stress fibres in association with focal adhesions (Pring *et al.*, 2003). Together, membrane protrusions, adhesion structures, and stress fibres work in concert to enable directed migration. Furthermore, ABPs are also critical for proper actin remodelling during migration (Alberts *et al.*, 2008).

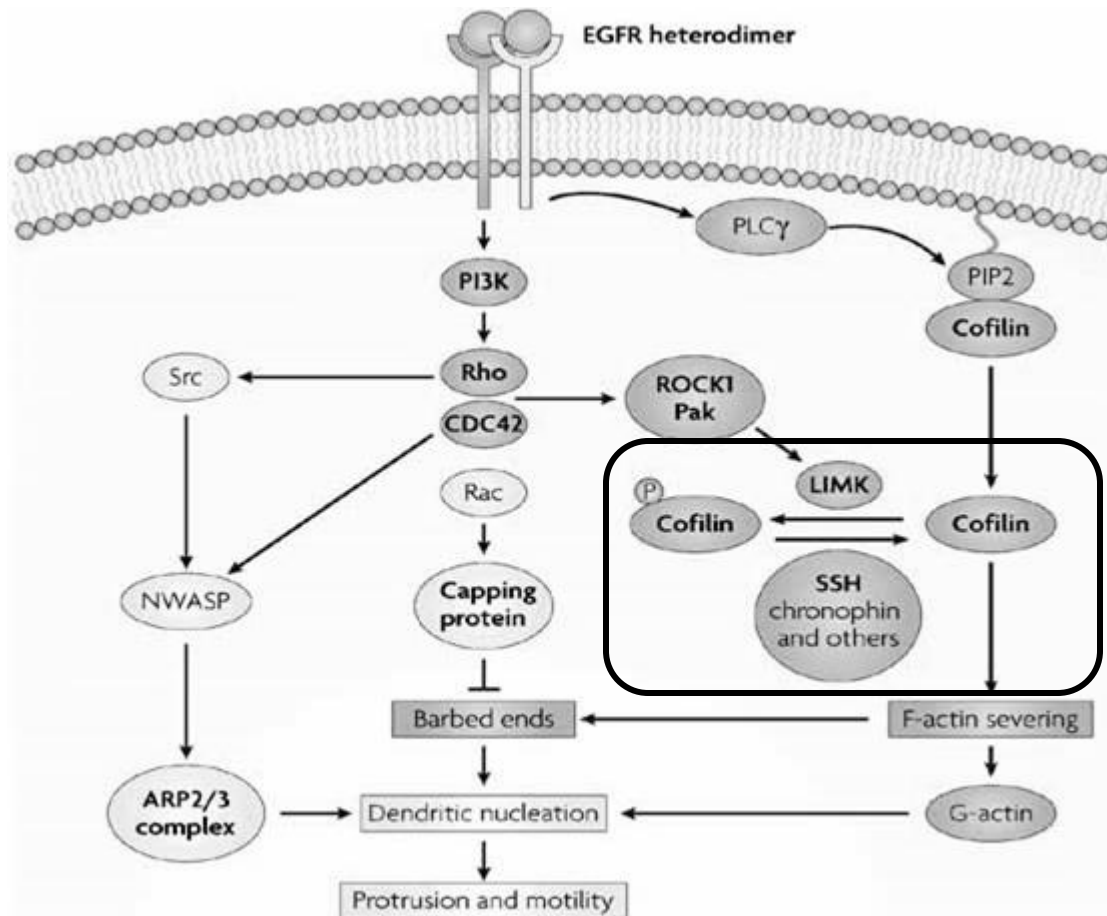
### **The Role of Cofilin during Cell Migration**

Cofilin plays a key role in rearranging actin architecture, which is necessary for directed cell migration. At the leading edge of the cell where Arp2/3-mediated actin networks form, cofilin severing of actin produces new barbed ends. Severing stimulates new filament elongation, thus contributing to the formation of membrane protrusions (Figure 1.1). Here, cofilin also works to depolymerize aged actin filaments, and recycle the subunits for rapid network formation (Zebda *et al.*, 2000).

Directed migration via actin rearrangement is activated through signal transduction cascades. These pathways are initiated by the binding of growth factors to their extracellular receptors. Figure 1.2 depicts the EGF-induced pathway that regulates cofilin and actin-based migration. Inside the cell, phosphoinositide-3-kinase (PI3K) is activated, which then stimulates downstream RhoGTPases such as Rho, Rac, and Cdc42. Rho governs assembly of stress fibres, while Rac and Cdc42 pathways regulate lamellipodia and filopodia formation, respectively (Yamazaki *et al.*, 2005). With regard to cofilin regulation, RhoGTPases activate Rho-associated coil-coil-forming kinase (ROCK). When ROCK is inhibited, filamentous actin aggregates within the cell and focal adhesion and membrane protrusion formation increases (Hopkins *et al.*, 2007). This coincides with ROCK's function as a regulator of downstream LIM-kinase (LIMK). LIMK becomes active when phosphorylated at certain threonine residues (Amano *et al.*,

2001; Ohashi *et al.*, 2002). In cells that have increased motility, expressing dominant negative forms of LIMK or creating knock-downs results in decreased locomotion (Yoshioka *et al.*, 2003; Suyama *et al.*, 2004). Importantly, LIMK inactivates cofilin by phosphorylating it on serine 3. Cofilin can be dephosphorylated, and thus activated, by a phosphatase called Slingshot (SSH). Knock down of SSH increases cofilin activity, causing multiple lamellipodia to form. Therefore, cofilin hyperactivity impairs directional migration (Nishita *et al.*, 2005). As suggested, the phosphorylation state of cofilin has a major impact on migration. When activated, cofilin can contribute to migration by severing and disassembling actin filaments at the leading edge of polarized cells (Nishita *et al.*, 2005; Hopkins *et al.*, 2006). Phosphorylated ADF/cofilin is not able to sever filaments or induce actin disassembly (Morgan *et al.*, 1993). Also, overexpression of LIMK increases cofilin phosphorylation, leading to a decrease in free barbed ends due to a lack of cofilin severing capabilities. Thus, actin polymerization at the leading edge ceases, and lamellipodia fail to develop (Zebda *et al.*, 2000; Samstag *et al.*, 2003).

In addition, cofilin is activated by another pathway. Although still unclear, evidence has shown that some cofilin is bound to phosphatidylinositol 4,5-bisphosphate (PIP<sub>2</sub>) at the plasma membrane. Cofilin is released and activated upon PIP<sub>2</sub> hydrolysis by phospholipase C (PLC) into diacylglycerol (DAG) and inositol 1,4,5-triphosphate (IP<sub>3</sub>) (Yonezawa *et al.*, 1990; Wang *et al.*, 2007; Alberts *et al.*, 2008). The PIP<sub>2</sub> and F-actin binding sites on cofilin overlap, suggesting that this PLC-mediated pathway regulates



Adapted from Wang *et al.* (2007)

**Figure 1.2: The cofilin regulation pathway.** Cofilin activity is controlled by EGF. EGF binds to and activates its receptor tyrosine kinase, which subsequently activates PI3K in the cytosol. PI3K has many downstream effectors, including RhoGTPases. During cofilin regulation, these effector proteins phosphorylate ROCK. Active ROCK can phosphorylate LIMK, which then inactivates cofilin by phosphorylating it. Phosphatases such as SSH dephosphorylate cofilin, therefore rendering it active and able to sever and disassemble actin filaments. EGF-binding can also activate cofilin through the PLC pathway. PLC hydrolyzes PIP<sub>2</sub> into IP<sub>3</sub> and DAG. Cofilin that was bound to PIP<sub>2</sub> is activated upon release.

actin-cofilin dynamics (Yonezawa *et al.*, 1990). Leyman *et al.* (2009) demonstrated that directional migration via lamellipodia formation was in fact regulated by sequestration and release of cofilin by PIP<sub>2</sub>. When cofilin was bound, protrusive activity was reduced. Ultimately, the two different cofilin activation pathways described, as well as the Arp2/3-mediated pathway, work simultaneously to promote directed cell migration (Yamaguchi and Condeelis, 2006).

### **The Role of Aip1/WDR1 during Cell Migration**

Aip1 and its homologues have been shown to interact with cofilin and cofilin-bound actin, which are essential to directional cell migration. Although the regulation and activation of Aip1/WDR1 is largely unstudied, a role in cell migration alongside cofilin is suspected. For example, while caspase-11 is generally a regulator of inflammatory and apoptotic events, it has been shown that migrational defects occur in caspase-11-null leukocytes. Caspase-11 appears to regulate Aip1/WDR1's interaction with cofilin by interacting with F-actin and Aip1/WDR1 to increase proximity to actin-bound cofilin. Coimmunoprecipitation assays revealed that the C-terminal propeller domain of Aip1/WDR1 directly interacts with the N-terminal CARD domain of caspase-11 (Li *et al.*, 2007).

There is considerable support for Aip1/WDR1's functional involvement in cell motility. In *Dictyostelium*, localization of DAip1 is specifically seen in anterior protrusions in cells stimulated or unstimulated by a chemotactic gradient. Locomotion in DAip1 wild-type cells is 46% faster than in DAip1-null cells. Also, despite DAip1 levels being higher when DAip1 is overexpressed in null cells compared to the wild-type, motility is approximately the same. Overall, DAip1 is necessary for cell motility (Konzok

*et al.*, 1999). In *Drosophila* S2 cells, Aip1 is required, along with cofilin, for actin remodelling involved in formation of lamella. When Aip1 is knocked-down, actin turnover is impaired (Rogers *et al.*, 2003). A study by Tsuji *et al.* (2009) established that elongation of actin responsible for lamellipodia expansion was dependent upon regulation of Aip1 barbed-end capping. Also, disruption of actin by Aip1 occurred faster than Arp2/3-mediated nucleation. Phalloidin staining of actin and fluorescent speckle microscopy showed that Aip1 was evenly distributed within the lamellipod structure, while Arp2/3 was more concentrated immediately at the leading edge. Together, this indicates that Aip1 promotes efficient actin turnover during migration simultaneously with actin nucleation mechanisms.

WDR1's involvement in directional migration has become apparent with recent evidence. In murine macrophage cells, knocking down WDR1 decreased migration rate in the presence and absence of macrophage chemoattractants. Formation of membrane ruffles, which are associated with migration, was lessened in these WDR1 knock-downs (Li *et al.*, 2007). In neutrophils with non-functional WDR1, F-actin levels increase, migration rates are reduced, and cofilin mislocalizes (Kile *et al.*, 2007). Furthermore, WDR1 expression is upregulated in chick basilar papilla after noise damage. Avian auditory hair cells are capable of regeneration, thus increased WDR1 in association with actin remodelling is likely due to necessary migration during cell repair processes (Lomax *et al.*, 2001). WDR1's localization patterns during cell migration further support its functional interactions. WDR1 is present at cell adhesion sites, becomes more concentrated in cortical regions at the leading edge during membrane protrusion

development, and becomes diffuse within the cell when actin-based migratory structures begin to disassemble (Noone and Hubberstey, unpublished).

### **Cancer and Metastasis**

Cancer is characterized by several general traits or behaviours. First, unrestrained cell proliferation occurs due to a disregard for regulatory mechanisms. Cells also avoid programmed cell death and differentiation to become immortalized. Genetic instability is necessary for cancer development as well, and is manifest as irreparable DNA damage or replication errors, or even as aberrant karyotypes. Finally, if cancer cells are defined as malignant, they are capable of invading their surrounding environment and will relocate. Malignancies are also able to fully metastasize and proliferate at foreign locations. The progression of invasion and metastasis is complex and requires highly-coordinated processes (Hanahan and Weinberg, 2000). In general, a tumour cell from the primary lesion must be able to invade and remodel the surrounding three-dimensional extracellular matrix (ECM). For successful invasion, tumour cells must develop invadopodia, podosomes, and lamellipodia. A defining characteristic of invadopodia is an increased ability to degrade and remodel the ECM (Yilmaz and Christofori, 2009). This is made possible through the upregulated expression of matrix metalloproteinases (MMP) such as MT1-MMP collagenase (Kelly *et al.*, 1998), and through MMP recruitment by actin-network formation near adhesion sites (Yilmaz and Christofori, 2009). Invasive cells must then intravasate into a blood or lymph vessel using the same principles for invasion into the ECM (Yamaguchi and Condeelis, 2006; Alberts *et al.*, 2008). Entrance into the circulation is critical, and is the next step that allows for potential metastasis to occur. Metastatic success is achieved if the circulating cells then extravasate out of

vessels and invade tissue or the ECM at another location. Relocated tumour cells also must proliferate by evading apoptosis and survive by recruiting blood vessels via angiogenesis (Hanahan and Weinberg, 2000).

Different types of malignant cancers have distinct invasive capabilities and individual metastatic profiles. Human MCF7 cells are derived from a pleural effusion that originated from a mammary gland adenocarcinoma. *In vitro*, MCF7 cells have relatively low invasive capabilities, most likely in part due to a lack of matrix metalloproteinases, although metastases are observed *in vivo*. These cells also retain many characteristics of the mammary epithelium, their originating tissue (Soule *et al.*, 1973). Another human cell line, Hs578T, is derived from a mammary ductal carcinoma. This line is highly invasive and metastatic *in vitro* and *in vivo* (Hackett *et al.*, 1977). Both of these breast cancer lines possess epidermal growth factor receptors (EGFR), which play a role in the signalling processes necessary for invasion (Smith, 1979; Bacus *et al.*, 1990; van Dijk *et al.*, 1997). MCF7 and Hs578T are the two breast cancer cell lines used as models for cell migration and invasion in this study.

### **Actin-based Cell Motility in Cancer**

Generally, cells become cancerous by exploiting normal, regulated cell machineries. These include pathways involved in proliferation, growth, cell death, and motility. In order for cancer cells to become malignant, regulatory mechanisms for cell motility are taken over to promote migration and invasion. Targeting the actin-based cytoskeleton is particularly important in this endeavour, as it is required for cell remodelling during normal directed migration. Using lamellipodia and filopodia, cancer cells can migrate two-dimensionally along the ECM. Podosomes, found in highly-motile

but noncancerous cell types, and invadopodia, seen in cancer cells, are required for actual invasion into the ECM and other three-dimensional substrates (Yamaguchi and Condeelis, 2006).

Like other membrane protrusions, invadopodia rely on extracellular chemotactic gradients to stimulate actin assembly, as well as the PI3K-RhoGTPase pathways that regulate Arp2/3 nucleation and cofilin activity. Cancer cells can self-stimulate by producing growth factors. In addition, a paracrine signalling loop is established between tumour-associated macrophages (TAM) that emit growth factors such as EGF, and tumour cells that attract TAMs by releasing chemokines such as colony-stimulating factor 1 (CSF1) (Yamaguchi *et al.*, 2006; Yilmaz and Christofori, 2009). PI3K plays a key role in cancer cell motility. Various types of cancers exhibit overexpression of PI3K or mutations that heighten its role as a kinase (Shayesteh *et al.*, 1999; Ma *et al.*, 2000). Moreover, inhibiting PI3K activity leads to decreased tumorigenicity (Lemke *et al.*, 1999; Hu *et al.*, 2000). Overexpression or hyperactivity of RhoGTPases, including Rho, Rac, and Cdc42, is also seen in many types of cancers such as breast, lung, and liver, and can lead to metastasis (Barber and Welch, 2006). There is plenty of evidence to also suggest that ROCK inhibition reduces the invasive ability of cancer cells (Hopkins *et al.*, 2007). Arp2/3-mediated actin nucleation and network establishment is crucial to both migration and invasion of cancer cells. Arp2/3 is distinctly present in invadopodia, and deregulation of its upstream effectors can interfere with a cell's invasive capabilities. When Cdc42 is knocked-down, Arp2/3 complex assembly is inhibited and leads to defective actin-network branching (DesMarais *et al.*, 2004; El-Sibai *et al.*, 2007).



Importantly, it has become clear that LIMK-cofilin and PIP<sub>2</sub>-cofilin regulation are essential for invasion and metastasis. Wang *et al.* (2006) provided evidence of LIMK and cofilin involvement in malignancies. When LIMK expression was increased in cancerous lung cells, invasion and metastasis was restricted. If cofilin was subsequently overexpressed in the same cells, malignant phenotypes were rescued. Furthermore, invadopodia were more transient and less invasive when cofilin levels were diminished (Yamaguchi *et al.*, 2005). Together this information strongly suggests that cancer cell motility is in direct relation to the regulation of cofilin phosphorylation (Wang *et al.*, 2006). On the contrary, PLC regulation of cofilin, and not cofilin phosphorylation status, may also be responsible for motility in cancer. Since the PLC-regulated pathway of cofilin activation is not well understood, the definitive role of this cofilin regulatory mechanism remains elusive. Despite this, information collectively demonstrates a necessity for cofilin in malignant cancers (Song *et al.*, 2006; van Rheenan *et al.*, 2007).

Finally, evidence is slowly emerging to support the role of Aip1/WDR1 in cancer cell motility. Mouse embryos transformed using insoluble nickel compounds exhibit differential expression of several genes, including WDR1, which is overexpressed. Typically, exposure to these compounds increases the risk of lung and nasal cancers (Landolph *et al.*, 2002). With regard to motility, the knock-down of Aip1 results in the reduction of chemotactic migration in lymphoma cells, and the formation of multiple membrane protrusions along the cell's perimeter. It is likely then, that Aip1 is not only essential for migration of cancer cells, but also for the directionality of the migration (Kato *et al.*, 2008).

## Summary

Evidence has implicated the regulation of cofilin activity as essential to cancer cell migration and invasion. Data suggest that Aip1/WDR1 may also be involved in cancer cell motility, although more information is needed for corroboration. Specifically, a correlation between WDR1 and invasion and metastasis has yet to be explored. Furthermore, the cofilin-WDR1 relationship is not fully understood. In addition, WDR $\Delta$ 35 is not well characterized and further exploration of its structure, localization, and function is imperative.

There are two main research objectives described in this thesis:

1. To examine the role of WDR1 isoforms in cancer cell migration and invasion
2. To clarify the relationship between WDR1 isoforms and cofilin in terms of expression and activation.

## **Chapter Two: Materials and Methods**

### **Cell Culture**

Hek293 (Human embryonic kidney 293 cells) and Hs578T cell lines were cultured in Dulbecco's modified Eagle's medium (DMEM), and MCF7 cells were cultured in RPMI-1640 medium. All media were supplemented with 10% fetal bovine serum (FBS) and 1% penicillin/streptomycin. Cell cultures were incubated at 37°C in a 5% CO<sub>2</sub> atmosphere. At approximately 90% confluency, cultures were sub-cultivated at a ratio of 1:2, 1:5, or 1:10 using trypsin-ethylenediaminetetraacetic acid (EDTA). All reagents were obtained from Sigma-Aldrich.

### **DNA Extraction**

Two millilitres of Luria-Bertani (LB) broth was inoculated with 10µl of *Escherichia coli* glycerol stock and incubated overnight (approximately 16hr) at 37°C. Twenty microlitres of overnight culture was used to inoculate 100ml LB, which was subsequently incubated overnight (approximately 16hr) at 37°C. Ampicillin or kanamycin was added to LB to a concentration of 100 µg/ml or 50µg/ml, respectively. Overnight cultures were then pelleted, and DNA was extracted using the GenElute HP Plasmid Maxiprep Kit from Sigma.

### **DNA Transfection**

Cells were grown to approximately 60-80% confluency prior to transfection, except for cells cultivated for the purpose of *in vitro* wound-healing scratch assays, which were grown to 100% confluency. For stable and transient transfections, plasmid DNA

constructs were transfected into Hek293, MCF7, and Hs578T cell lines using 2mg/ml sterile, filtered branched polyethylenimine (PEI; Aldrich) as a transfection reagent. For Hek293 and Hs578T cells, ~8 $\mu$ g of plasmid DNA was used, while ~16 $\mu$ g of plasmid DNA was used for MCF7 cells. First, in a separate reaction, DNA and PEI were added to the appropriate medium for each transfection. Then, after ~10min, this reaction was added to cells on a plate containing enough medium to dilute DNA and PEI to the specified concentrations. For stable and transient transfections, cells were given 24-36 hr to integrate and express the DNA before replacing the medium.

Specifically, for producing transient MCF7 cell lines, 16 $\mu$ g of either peGFP-C1, peGFP-WDR1, or peGFP-WDR $\Delta$ 35 plasmid DNA was transfected into cells. For transient Hs578T cell lines, 8 $\mu$ g of this plasmid DNA was transfected into cells. Expression of the GFP-fusion proteins was driven by a CMV promoter. Cells were tested for transfection efficiency by transfecting with various concentrations of PEI and of pCI- $\beta$ gal, a vector that constitutively expresses lacZ.

A second transfection method using Lipofectamine 2000 (Invitrogen) instead of PEI was used for Hek293 cells. In this case, 4-8 $\mu$ g of plasmid DNA, 10-20 $\mu$ l of Lipofectamine 2000, and serum-free medium (SFM) was used. After 4-6 hr of transfection, the medium was replaced with regular DMEM.

### **Stable Cell Line Selection**

MCF7 cells were transfected with pcDNA6/TR vector (Invitrogen) containing the reverse tetracycline transactivator gene driven by a CMV (Cytomegalovirus) promoter, as well as the blasticidin resistance gene. Cells were selected with 10 $\mu$ g/ml blasticidin (Invivogen). To confirm expression of the vector, cells were cotransfected with

pcDNA4/TO/lacZ vector (Invitrogen) containing a lacZ gene and tetracycline operator driven by a CMV promoter. Cells were stained using potassium cyanide (KCN) and X-gal (Fisher Scientific).

MCF7 cells that successfully integrated the pcDNA6/TR vector were cotransfected with pcDNA4/TO vector (Invitrogen). This vector contained either a GFP, GFP-WDR1, or GFP-WDR $\Delta$ 35 gene, and a tetracycline operator, with expression being driven by a CMV promoter. Cotransfected MCF7 cells were also selected with 75  $\mu$ g/ml zeocin (Invivogen). Several colonies were selected from the total population of cotransfected cells on a 10cm plate. Colonies were mechanically removed with a pipette, and were transferred to a 24-well plate containing ~200  $\mu$ l of trypsin-EDTA. After ~1 min of trypsinization, 1 ml RPMI was added to stop the reaction. Each colony was grown to confluency before being trypsinized and transferred to a 60mm plate, and eventually again to a 10cm plate. To induce expression of GFP-tagged genes, 1  $\mu$ g/ml doxycycline, or dox (Invivogen), was introduced into the medium for at least 18-24 hr.

For TREX cells (Hek293 cells expressing the reverse tetracycline transactivator), either pcDNA4/TO/lacZ or pcDNA4/TO vector was transfected. Stable cells were selected with 25  $\mu$ g/ml blasticidin, 150  $\mu$ g/ml zeocin, and by using the same colony selection process described for stable MCF7 cell lines.

### **X-gal Staining of Mammalian Cells**

After at least 24hr, cells transfected with either pcDNA4/TO/lacZ or pCI- $\beta$ gal vector were rinsed twice with 1x phosphate-buffered saline (PBS). Cells were then fixed using 0.05% glutaraldehyde (Sigma) for 5-10 min, and rinsed again three times with 1xPBS. Then 20mg/ml X-gal was added to KCN solution (0.164% w/v ferrocyanide,

0.211% w/v ferricyanide, 1M MgCl<sub>2</sub>) at a ratio of 1:20, and 1-2ml was added to fixed cells for at least 24 hr. Cells were then examined for X-gal (blue) staining using an inverted bright field microscope (Axiovert 25, Zeiss). To preserve stained cells, X-gal-KCN solution was removed and 1-2ml of 80% glycerol was added.

### **Protein Extraction**

Cells were grown to approximately 80-90% confluency before extraction. Cells used for EGF time courses were extracted at a slightly lower density to ensure cofilin-related cellular processes were not hindered by proximity of adjacent cells. Cells were rinsed twice with 1xPBS. For cells on 60mm plates, 160-250µl of radioimmunoprecipitation assay (RIPA) buffer (150mM NaCl, 0.1% sodium dodecyl sulphate (SDS), 50mM Tris-pH 7.4, 1% NP-40 (IGEPAL CA-630; Sigma), protease inhibitor cocktail tablet; Roche) was added after media was aspirated. After mechanical removal from the plate, the cell-RIPA solution was pulse-sonicated using a sonic dismembrator (Fisher Scientific) for ~30sec. Cellular debris was pelleted at 10000 rpm for 2min, and the protein supernatant was stored at -20°C.

### **Immunoblotting**

Total protein extracts were denatured in 1x Laemmli sample buffer by boiling for approximately 3min. Protein samples were separated by SDS-PAGE (sodium dodecyl sulphate – polyacrylamide gel electrophoresis) on a 10% or 12% polyacrylamide gel in 1x running buffer (25mM Tris-HCl, 250mM glycine-pH 8.3). A pre-stained protein ladder (Fermentas) was used as a marker.

Protein was blotted onto a nitrocellulose membrane (Fisher Scientific) in a Bio-Rad transfer apparatus containing 1x transfer buffer (25mM Tris-HCl, 192mM glycine-

pH 8.3, 20% methanol) at 4°C for approximately 1 hr. The membrane was incubated in 5% blocking solution (5% w/v fat-free skim milk powder in 1xTris-buffered saline with Tween 20 (TBST)) for at least 1 hr. Primary antibody incubation followed in either 1xTBST (Tris, NaCl, 0.05% Tween 20) for 1 hr or in primary dilution buffer (5% bovine serum albumin (BSA), 0.1% Tween 20, 10% TBS) overnight at 4°C. The membrane was rinsed 3x5min with 1xTBST followed by a 1 hr incubation with a horseradish peroxidase (HRP)-conjugated secondary antibody in either 1xTBST or secondary blocking solution (5% w/v fat-free skim milk powder, 0.1% Tween 20, 10% TBS). For a description of all primary and secondary antibodies used, see Appendix A. For a loading control, samples were probed with an anti-glyceraldehyde-3-phosphate dehydrogenase (GAPDH) antibody. The membrane was again rinsed 3x5min with 1xTBST before visualizing proteins using Lumi-light Western blotting substrate (Roche). AlphaEase FluorChem HD2 software and camera apparatus (AlphaInnotech) were used to expose the membrane and perform densitometric analysis. Densitometry output data was further analyzed using Microsoft Excel.

### **Immunofluorescence**

Cells transfected with HA (hemagglutinin) constructs were plated onto sterile 16mm round glass coverslips (CS; Fisher) and grown until approximately 50-60% confluent. CS were immersed in 3.7% formaldehyde solution in 1xPBS for 10min. CS were then incubated in 0.5% Triton X-100 for 10min, followed by a 2min wash in 1xPBS. Cells were then covered in 40µl of 1:200 anti-HA (12CA5) primary antibody and incubated for 30min at 37°C. Cells on the CS were then washed in 0.05% Tween 20 for 10min before incubating with 40µl of 1:200 Alexa Fluor 488 goat anti-mouse secondary

antibody (Molecular Probes) for 30min at 37°C. Again, CS were washed in 0.05% Tween 20 for 10min, then were rinsed in 1xPBS for 5min before briefly rinsing several times in ddH<sub>2</sub>O. CS were mounted on slides using anti-fade reagent, then sealed after 24hr before observing cells under a fluorescent microscope.

For visualizing cells expressing GFP, cells on CS were immersed in 3.7% formaldehyde solution in 1xPBS for 10min, then rinsed in 1xPBS for 2min. CS were briefly washed in ddH<sub>2</sub>O several times and mounted as described above.

### **EGF Induction Time Course**

Cells were grown to approximately 70-80% confluency before EGF induction and serum-starved for ~3hr. MCF7 cells were stimulated with 5ng/ml EGF (Sigma) in SFM, and Hs578T cells with 10ng/ml in SFM, for 0sec, 30sec, 1min, 2min, 5min, and 15min. EGF-SFM was aspirated and protein or RNA was then extracted from cells according to specified protocols.

### **RNA Extraction**

Cells were grown to approximately 80-90% confluency before extraction. As was done for protein extractions, cells used for EGF time courses were extracted at a slightly lower density. Cells were first rinsed with 1xPBS. Approximately 250µl of 1% 2-mercaptoethanol in lysis buffer (Sigma) was added to each 60mm plate of cells on ice. Cells were mechanically removed from plates using a cell scraper, and total RNA was extracted using the Sigma GenElute Mammalian Total RNA Miniprep kit. RNA aliquots were stored at -80°C.



## **RT-PCR**

RNA was converted to cDNA using the High Capacity cDNA Reverse Transcription kit from Applied Biosystems. Each reaction contained 1  $\mu$ l reverse transcriptase, 2  $\mu$ l random primers, 2  $\mu$ l 10x reverse transcription buffer, 0.8  $\mu$ l dNTP mix, 4.2  $\mu$ l ddH<sub>2</sub>O, and approximately 10  $\mu$ l of total RNA extract. A 2720 Thermal Cycler (Applied Biosystems), set at 25°C for 10min, 37°C for 120min, and 85°C for 5min, was used to carry out the reaction. cDNA samples were stored at -20°C.

## **Quantitative Real-Time PCR**

Each duplex qRT-PCR (quantitative real-time polymerase chain reaction) reaction contained 1  $\mu$ l GAPDH control primer-probe mixture, 1  $\mu$ l target primer-probe mixture, 10  $\mu$ l TaqMan gene expression analysis master mix, 7  $\mu$ l ddH<sub>2</sub>O, and 1  $\mu$ l cDNA, per well. Target primer-probes used included *H. sapiens* cofilin, WDR1, and WDR $\Delta$ 35. To ensure specificity, the WDR1 primer-probe set was designed against the exon 3-4 junction, while the WDR $\Delta$ 35 primer-probe set was designed across the exon 2-6 junction. All reagents used were from Applied Biosystems. Each cDNA sample reaction was run in triplicate within the same plate. Transcriptional expression analysis was then performed using the 7300 Real Time PCR System and Sequence Detection Software from Applied Biosystems. This software determined the relative quantification (RQ) values of gene expression by calculating the  $\Delta\Delta C_T$  values. Output data was further analyzed using Microsoft Excel, where the log of the RQ values were calculated (logRQ).

## **Wound Healing Assay**

Cells were plated onto gridded coverslips (Millennium Sciences, Inc.), displaying a 1 mm x 1 mm grid, divided into 100  $\mu$ m units. At 90% confluency, cells were transfected

and given 24-36hr to transiently express the appropriate GFP-fusion protein. A small wound, or scratch, was created mechanically in the fully confluent monolayer using a pipette tip, which uncovered 3-5 units across the grid. At 0hr, 12hr, 24hr, and 48hr, images of the wound and surrounding expressing and non-expressing cells were taken using a fluorescent microscope (CX41, U-RFLT50, Olympus) with QCapture Pro imaging software, and using a confocal microscope (IX81, Olympus) with FluoView software. For cells imaged using confocal microscopy, glass-bottom culture dishes (MatTek Corporation) with high optical clarity were used without gridded coverslips.

For cells grown on the CS, rate of migration was determined by using the microscopic grid to measure the width of the closing wound at several time points. Using the 100 $\mu$ m unit-grid, average total distance travelled by the cells was determined at 0, 12, 24, and 48hr by counting the number of visible grid squares across the wound several times per plate. Migration rate ( $\mu$ m/hr) for each plate of cells was calculated by dividing this average total distance travelled by total time (48hr). Wound-healing assays were repeated three times for each GFP-fusion protein cell line, and the final migration rate was then calculated by taking the average of the migration rate from each replicate.

### **Invasion Assay**

The CytoSelect 24-well cell invasion assay (Cell Biolabs, Inc.) was used to carry out invasion experiments and analysis. First, cells were given 24-36hr to transiently express the appropriate GFP construct. Cells were then allowed to grow on 60mm culture dishes to a concentration of  $0.5-1.0 \times 10^6$  cells/ml and serum-starved for ~3hr. This cell suspension in SFM was then added to the top section of a cell culture insert lined with basement membrane. To the lower chamber containing the insert, media containing 10%

FBS was added. This media also contained either 5ng/ml EGF for MCF7 cells or 10ng/ml EGF for Hs578T cells to further stimulate invasion. Cells were incubated at 37°C in 5% CO<sub>2</sub> atmosphere for 24-48hr to allow for invasive cells to move through the basement membrane. Cells that did not invade the membrane were removed. Invasive cells were then stained and extracted from the bottom of the cell culture insert. The optical density (OD) at 590nm was measured using a microplate reader and Workout software (Perkin Elmer Life Sciences). Cell extraction solution was used as a blank measurement. Two OD<sub>590</sub> measurements were taken for each repeat of each sample. Output data was further analyzed using Microsoft Excel.

## Chapter Three: Results

### Stable MCF7 cell line generation to express WDR1 proteins

In order to study the effects of WDR1 and WDR $\Delta$ 35 on various cell functions, these genes were overexpressed in a variety of mammalian cell lines. For stable overexpression, a tetracycline-inducible expression system was implemented in Hek293 cells. GFP-tagged WDR1 or WDR $\Delta$ 35 was co-expressed in Hek293 cells that already expressed a reverse tetracycline transactivator gene (TREX cells). GFP-WDR1 and GFP-WDR $\Delta$ 35 were stably integrated and expressed to create two individual cell lines. A GFP-expressing control cell line was also created. Western blot analysis determined that expression levels of GFP-WDR1, GFP-WDR $\Delta$ 35, and the GFP control were upregulated in the presence of doxycycline (a tetracycline derivative). Minimal expression was observed in the absence of doxycycline which arose due to leakiness of the expression system. These results confirmed that the inducible expression system can function properly in a human cell line in order to express GFP-tagged genes of interest (Figure 3.1).

For these studies, MCF7 cells that stably expressed GFP-tagged WDR1 or WDR $\Delta$ 35 were attempted. However, setting up the same tetracycline-inducible expression system in MCF7 cells to achieve stable expression of GFP-fusion proteins proved to be largely unsuccessful. In the first attempt to create stable MCF7 cell lines, it was discovered that the MCF7 cells being used were not of human origin (data not

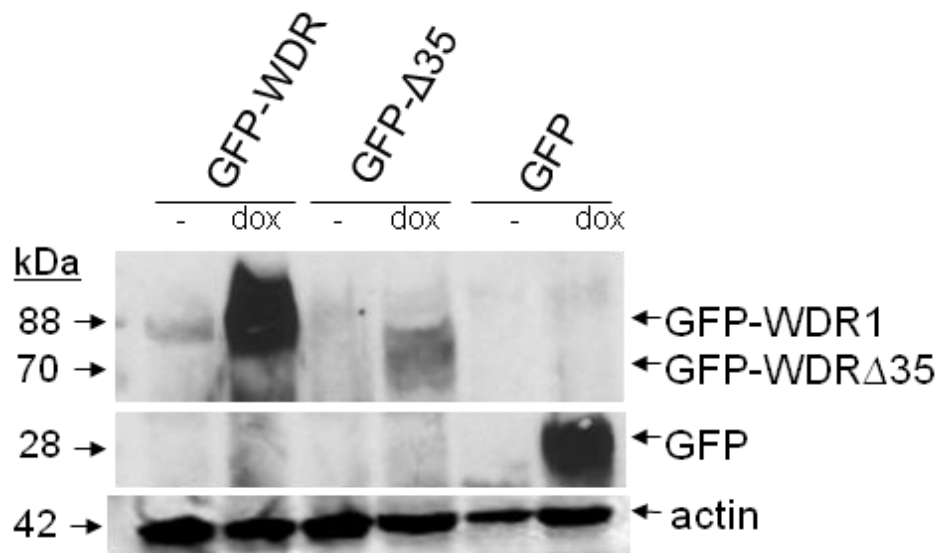


**Figure 3.1: Stable GFP fusion proteins can be inducibly expressed in Hek293 cells.**

GFP (control), or GFP-tagged WDR1 or WDR $\Delta$ 35 were stably integrated into Hek293 cells containing the reverse tetracycline transactivator gene (TREX cells), and were overexpressed using a tetracycline-on inducible expression system. Expression of GFP-WDR1 (88kDa), GFP-WDR $\Delta$ 35 (70kDa), and GFP (28kDa) in the presence (dox) or absence (-) of doxycycline was analyzed by Western blotting. Actin was used as a loading control.

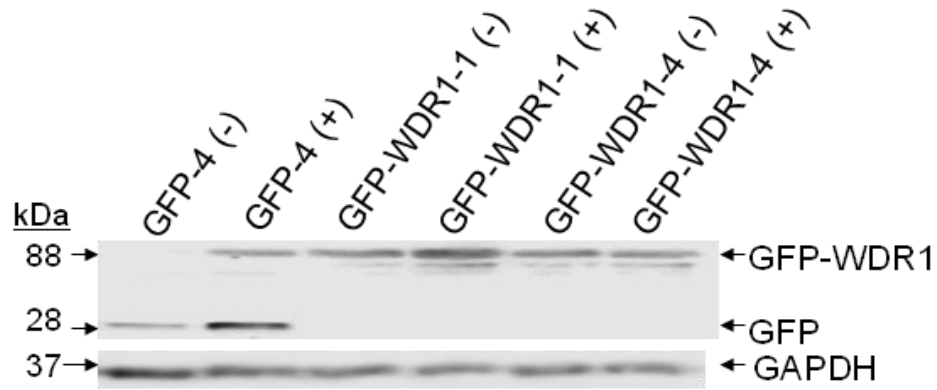
shown). qRT-PCR analysis verified that the original cells in question were undoubtedly of rodent origin, implying that these were in not MCF7 cells (data not shown). Since the cell type of these potentially-stable cells was not identified, they were terminated. The results of the second attempts are shown in Figures 3.2 and 3.3. Western blotting was used to screen various MCF7 lines that potentially expressed the GFP, GFP-WDR1, or GFP-WDR $\Delta$ 35. Densitometric analysis was performed to quantify expression levels that were normalized to GAPDH. Although one GFP control line (GFP-4) showed successful stable integration, stable lines expressing GFP-WDR1 and GFP-WDR $\Delta$ 35 could not be generated (Figure 3.2). Despite the relative expression levels of doxycycline-induced GFP-WDR1-1 and GFP-WDR1-4 being upregulated, repeated Western blotting and immunofluorescence could not confirm inducible expression. Furthermore, HA-tagged WDR1 or WDR $\Delta$ 35 fusion proteins were introduced into MCF7 cells expressing the reverse tetracycline transactivator gene. Western blotting (Figure 3.3) and immunofluorescence (not shown) revealed that none of the cell lines potentially expressing either of the HA fusion proteins were stable. Overall, these results indicated that only one MCF7 stable cell line was created containing GFP, which was not sufficient for further analysis, therefore transient transfections were employed.

### **GFP-fusion proteins are transiently expressed and maintained in MCF7 and Hs578T cells**

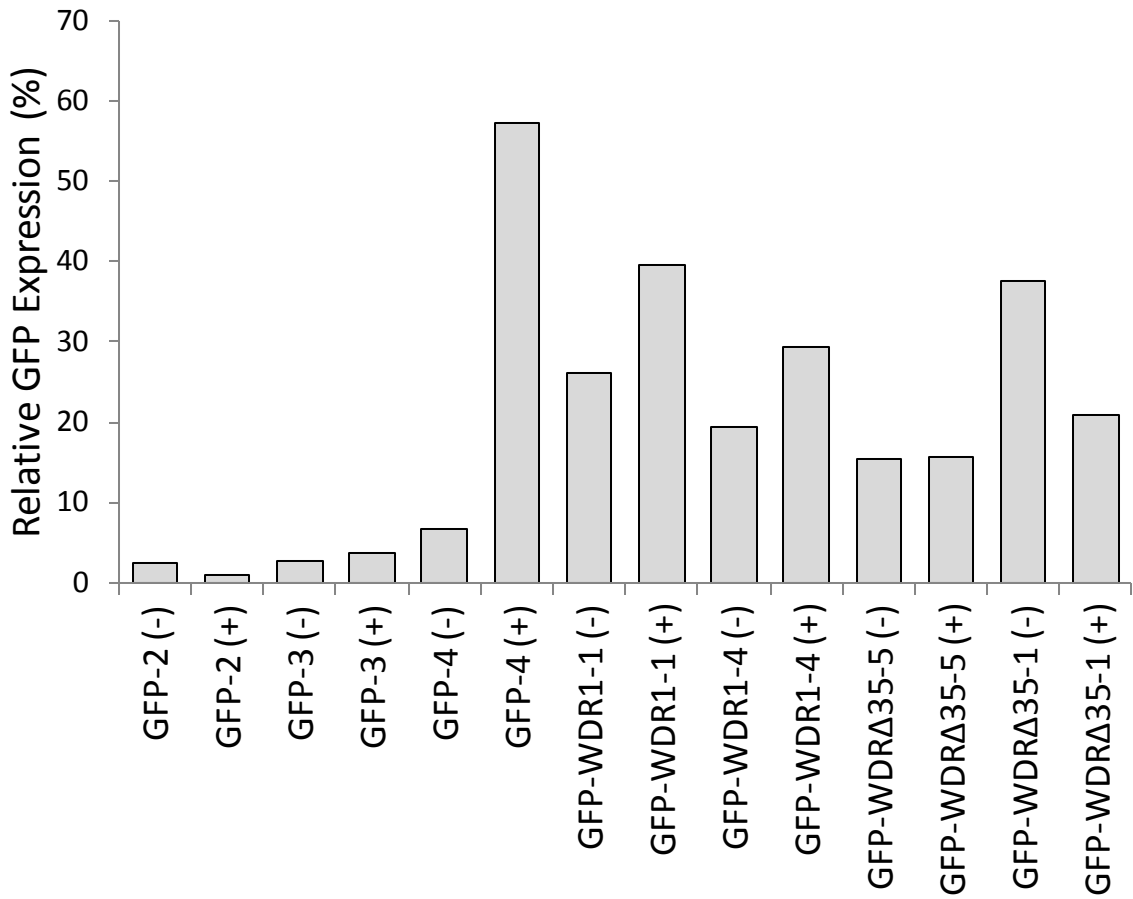
Since stable breast cancer cell lines could not be established, it was therefore necessary to transiently express GFP, GFP-WDR1, or GFP-WDR $\Delta$ 35 in different cancer cell lines. To examine the effects of overexpression in cancer cell lines with different

**Figure 3.2: Only one stable MCF7 cell line, GFP-4, was successfully created.** (A) MCF7 cells expressing the reverse tetracycline transactivator gene were transfected with GFP, GFP-WDR1, or GFP-WDR $\Delta$ 35 to create potentially-stable cell lines. Each cell line was then induced with doxycycline (dox). Western blot analysis using a GFP antibody was used to detect GFP expression and screen these potentially-stable cell lines in the presence (+) or absence (-) of doxycycline. (B) Induced expression of GFP-fusion proteins was quantified using densitometry and compared to quantified levels of uninduced GFP-fusion protein expression. GFP, GFP-WDR1, and GFP-WDR $\Delta$ 35 expression values were normalized to GAPDH (loading control) expression values to determine relative expression levels.

A



B





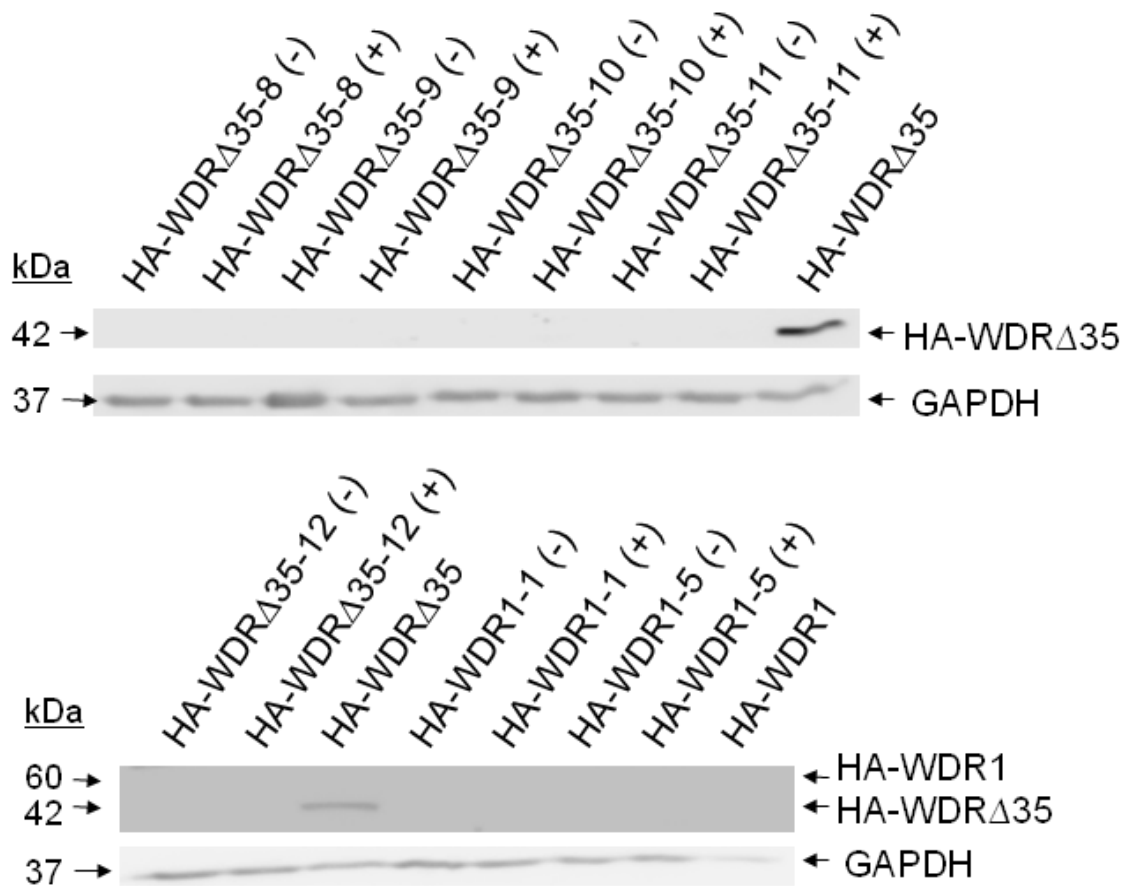


**Figure 3.3: No stable HA MCF7 cell lines were successfully created.** Establishing MCF7 cells stably expressing HA-WDR1 (60kDa) or HA-WDRΔ35 (42kDa) instead of GFP-fusion proteins was attempted using the same inducible expression system. Each cell line was induced with doxycycline (dox), and Western blot analysis was used to screen these potentially-stable cell lines in the presence (+) or absence (-) of doxycycline. Cells that constitutively overexpressed HA-fusion proteins (HA-WDR1 and HA-WDRΔ35) were used as positive controls for expression. GAPDH was used as a loading control.

invasive properties, both MCF7 and Hs578T breast cancer lines were chosen. To test the endurance of transient GFP expression in a cell line, MCF7 cells were transfected with GFP control, GFP-WDR1, or GFP-WDR $\Delta$ 35. Images of expressing cells were captured every 24hr over a seven day period. Figure 3.4 shows that GFP expression remained relatively constant for up to 96hr for the GFP control, and up to 72hr for GFP-WDR1 and GFP-WDR $\Delta$ 35 cell lines. Expression levels noticeably declined after these particular time points and remained low. This result confirmed that expression of a transiently transfected GFP-fusion protein endured within the cell for a length of time suitable for examining migration, invasion and the cofilin-WDR1 relationship.

To verify that these GFP-fusion proteins were indeed being transiently expressed, Western blot analysis was necessary. GFP, GFP-WDR1, and GFP-WDR $\Delta$ 35 could all be individually expressed in MCF7 (Figure 3.5A) and Hs578T cells (Figure 3.5B), although at different expression levels. Expression levels of GFP-WDR1 and GFP-WDR $\Delta$ 35 were noticeably lower than the control. Along with MCF7 imaging, fluorescent confocal imaging of GFP, GFP-WDR1, and GFP-WDR $\Delta$ 35 expression in Hs578T cells confirmed the expression patterns seen with Western blotting. Approximately 30% of transfected cells expressed GFP-WDR1 or GFP-WDR $\Delta$ 35.

### **WDR1 or WDR $\Delta$ 35 overexpression does not affect migration rate or invasiveness**

Recent findings suggest that Aip1/WDR1 is involved in cancer cell migration and directionality, but its role has not been fully explored (Landolph *et al.*, 2002; Kato *et al.*,

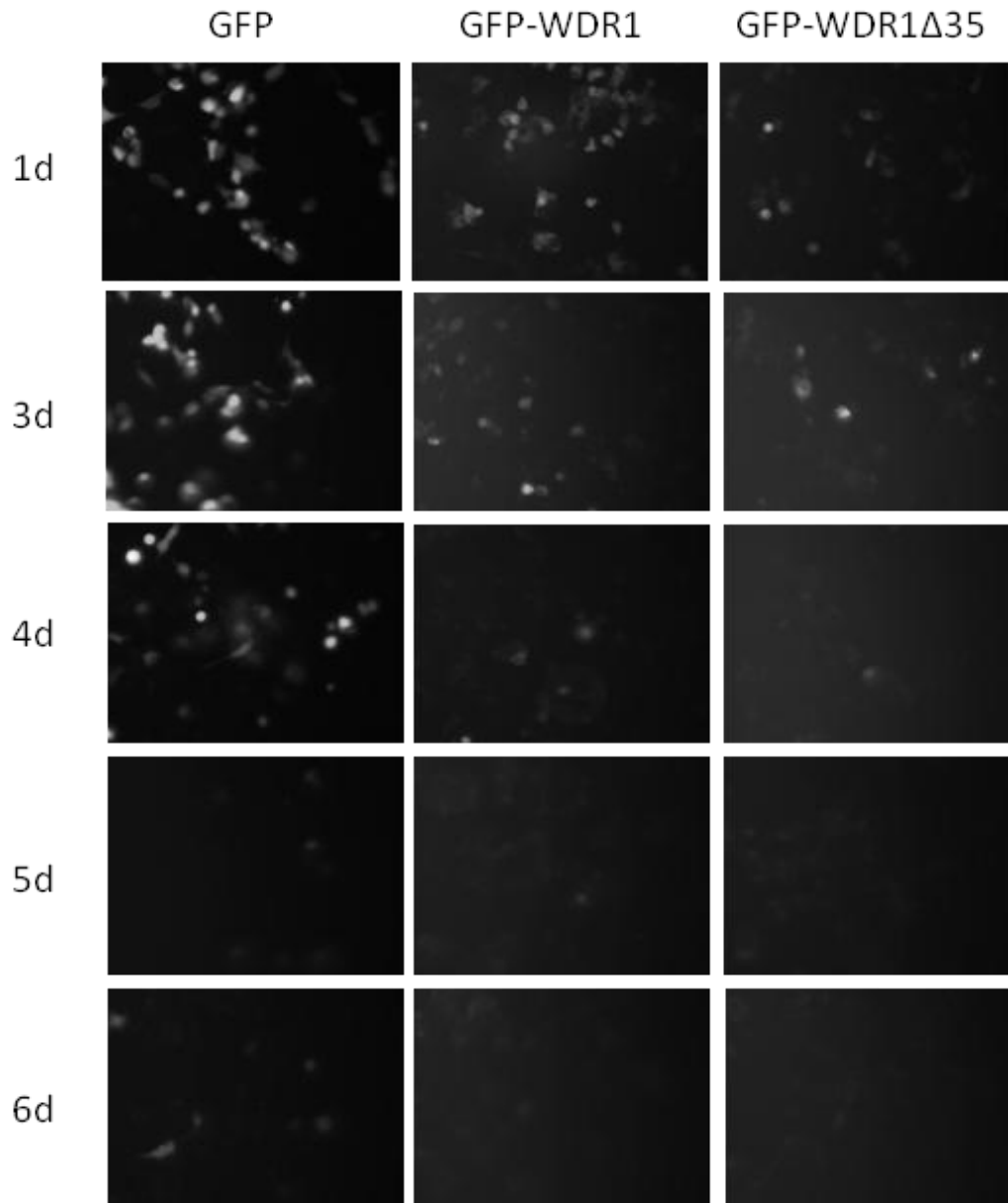
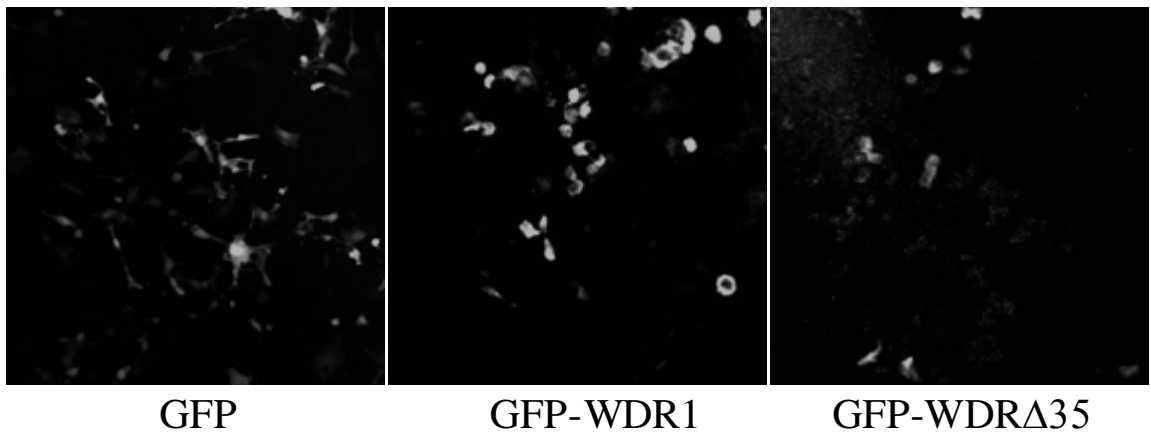
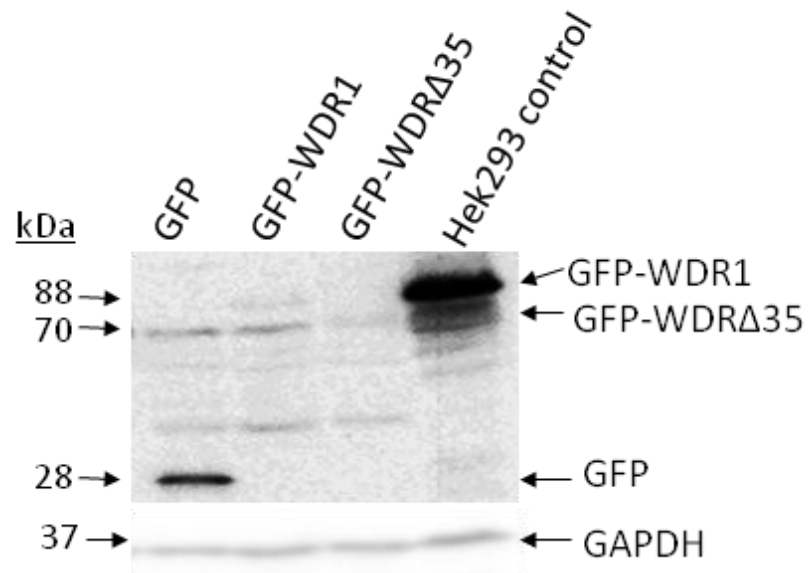


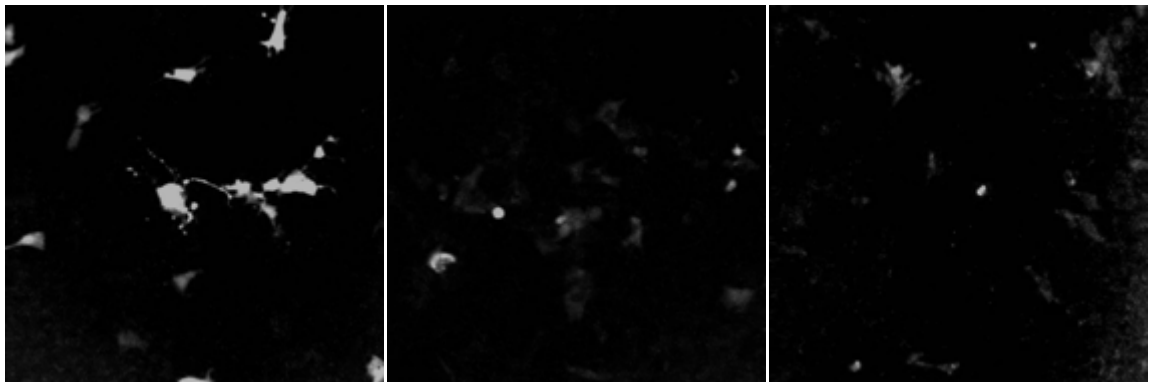
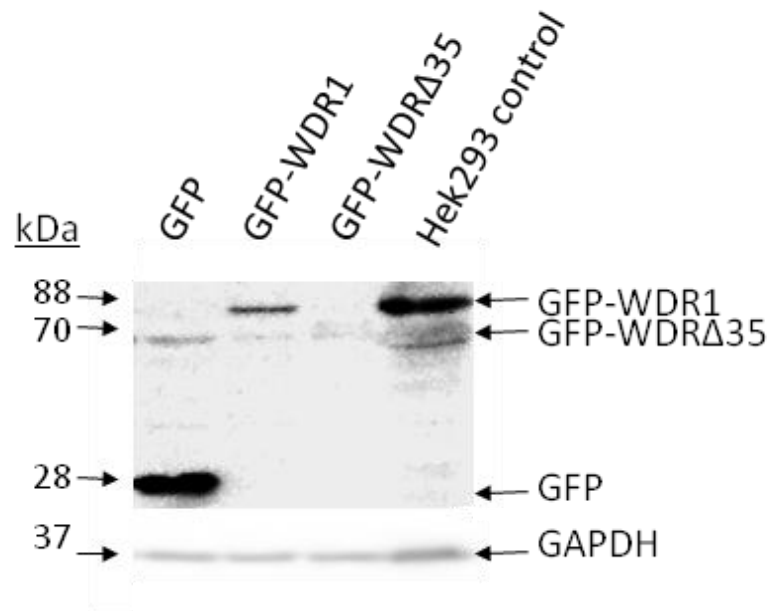
**Figure 3.4: GFP-WDR1 and GFP-WDR $\Delta$ 35 maintained consistent levels of transient expression for up to 72hr.** MCF7 cells were transiently transfected with GFP, GFP-WDR1, or GFP-WDR $\Delta$ 35 to achieve temporary overexpression of the GFP-fusion proteins. GFP-fusion protein expressing cells were examined after every 24hr over a 7d period. At each 24hr time point, fluorescent images of live cells were taken to determine how long expression would endure.

**Figure 3.5: GFP-WDR1 and GFP-WDR $\Delta$ 35 are expressed in MCF7 and Hs578T cells after transient transfection.** Using Western blot analysis, a GFP antibody detected GFP and GFP-tagged WDR1 and WDR $\Delta$ 35 expression in (A) MCF7 and (B) Hs578T cell lines. As a positive control for GFP-fusion protein expression, Hek293 GFP-WDR1 (dox) and Hek293 GFP-WDR $\Delta$ 35 (dox) samples were combined in the same lane (TREX control). GAPDH was used as a loading control. Fluorescent confocal images were taken to examine GFP-fusion protein expression in MCF7 and Hs578T cells *in vitro*.

A MCF7



B Hs578T



GFP

GFP-WDR1

GFP-WDR $\Delta$ 35

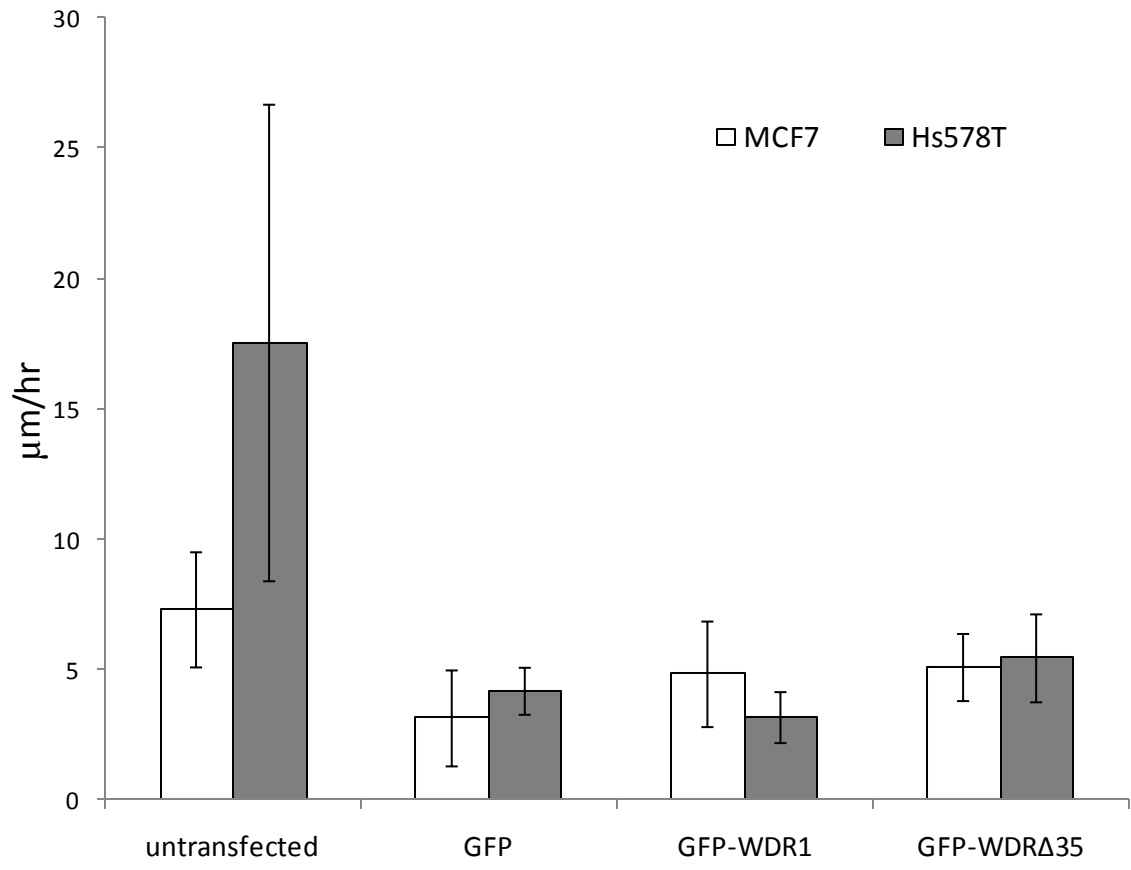
2008). As well, the function of WDR $\Delta$ 35 has not been studied, therefore it was necessary to determine the effects of overexpressing WDR1 or WDR $\Delta$ 35 on migration rate.

Before performing *in vitro* wound-healing scratch assays, cells were transiently transfected with GFP, GFP-WDR1, or GFP-WDR $\Delta$ 35. Migrating cells at the wound edge were imaged and measured at 0, 12, 24, and 48hr. These assays revealed that overexpression of WDR1 or WDR $\Delta$ 35 in 30% of MCF7 or Hs578T cells did not significantly affect rate of migration compared to the migration rate of GFP control cells (Figure 3.6A). Also, there was no significant difference in migration rate between WDR1- and WDR $\Delta$ 35-overexpressing cells. Finally, MCF7 and Hs578T cell lines expressing GFP-fusion proteins did not exhibit any difference in migration rate compared to one another, however untransfected Hs578T cells migrated significantly faster than untransfected MCF7 cells. Fluorescent confocal imaging of migrating MCF7 cells over 48hr demonstrated that cells with upregulated WDR1 expression did not migrate faster. Approximately 1.6% of cells overexpressed GFP-WDR1 near the wound edge compared to 8% overexpressing GFP after 48hr, suggesting that WDR1 may actually slow migration. However, 15.52% of cells overexpressed GFP-WDR $\Delta$ 35 at the wound edge. Thus, MCF7 cells expressing GFP-WDR $\Delta$ 35 appeared to migrate faster than surrounding control cells after 48hr (Figure 3.6B). Confocal microscopy also revealed that expressing GFP-WDR1 in Hs578T cells increased migration rate compared to surrounding non-expressing control cells after 12hr, when 12.5% of cells at the wound edge were overexpressing compared to only 4.89% of GFP-expressing cells in the control (Figure 3.6C). This trend continued at 24hr and 48hr, with 33.75% and 43.52% of cells

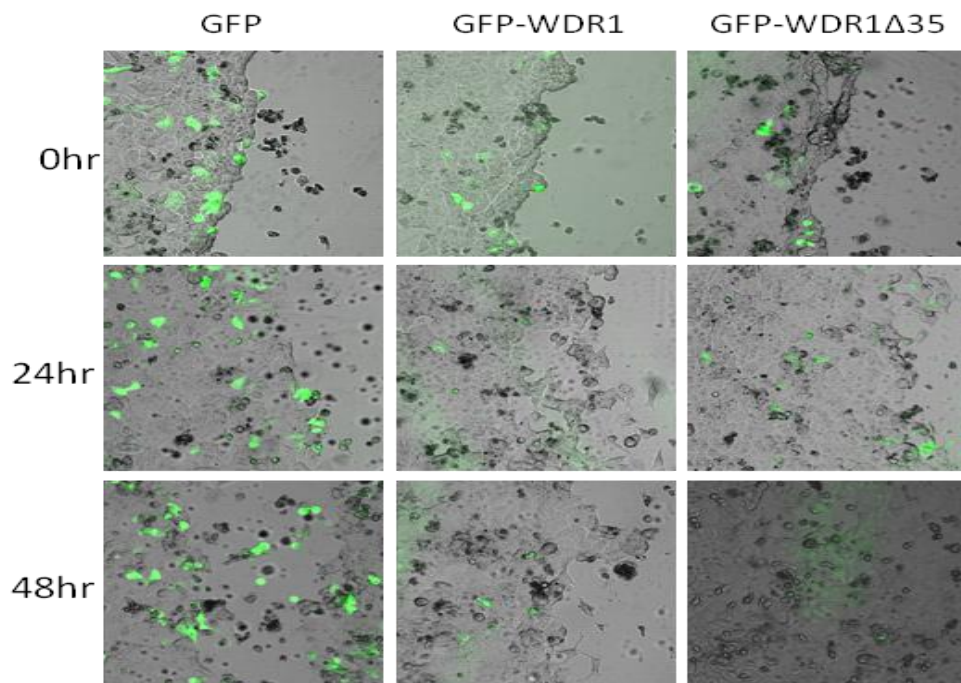
**Figure 3.6: Transient overexpression of WDR1 isoforms does not significantly affect migration rate of MCF7 or Hs578T cells.** (A) Wound-healing assays were used to determine the average migration rate of MCF7 and Hs578T cell lines transiently expressing GFP-WDR1 or GFP-WDR $\Delta$ 35 over a 48hr timecourse. Distance of migration was measured at 0, 12, 24, and 48hr using a microscopic grid. Average total distance travelled was determined by counting the number of visible grid squares across the wound several times per plate, where each square was equal to 100  $\mu$ m. Migration rate ( $\mu$ m/hr) for each plate of cells was calculated by dividing this average total distance travelled by total time (48hr). Migration rate for each GFP-fusion protein cell line was then calculated by taking the average of the migration rates calculated for each replicate. (B-C) Imaging of (B) MCF7 and (C) Hs578T cell lines expressing GFP, GFP-WDR1, or GFP-WDR $\Delta$ 35 was done over the 48hr time course using a confocal microscope (shown) and a fluorescence microscope.



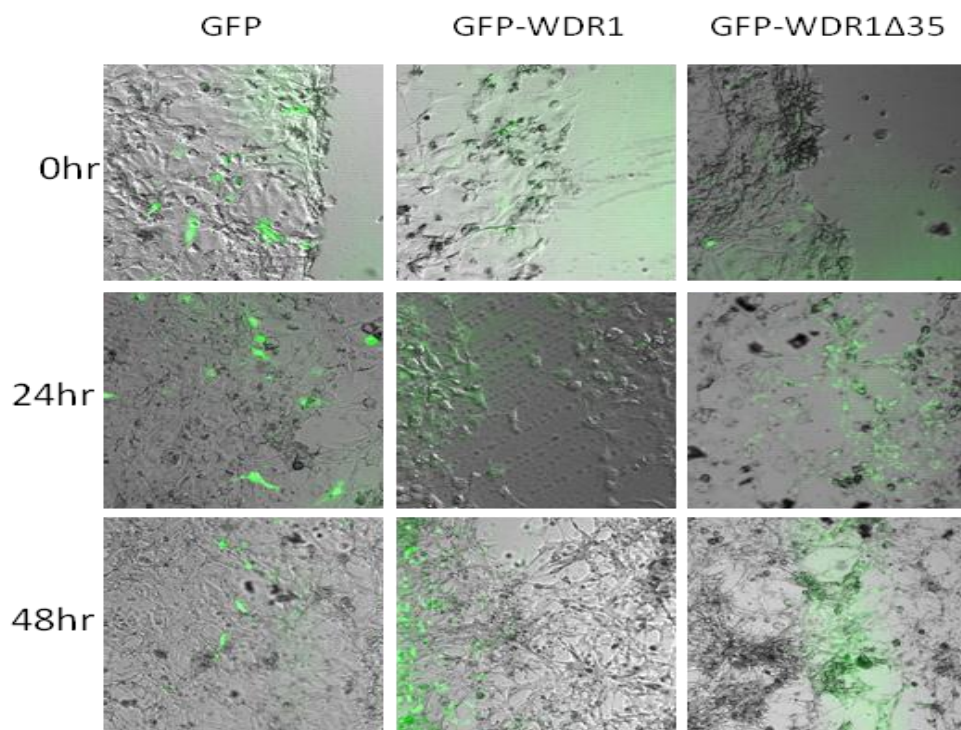
A



**B MCF7**



**C Hs578T**



overexpressing GFP-WDR1, respectively. Also, cells overexpressing GFP-WDR $\Delta$ 35 clearly migrated into the wound faster than surrounding control cells and at faster rates than cells expressing GFP-WDR1. At the wound edge, approximately 44.05%, 65.48%, and 56.73% of cells were overexpressing GFP-WDR $\Delta$ 35 after 12hr, 24hr, and 48hr, respectively. These observations suggest that in MCF7 and Hs578T cells, WDR1 and WDR $\Delta$ 35 may play a regulatory role during migration. Along with previous evidence supporting a role for Aip1/WDR1 in cell migration, these results suggest that WDR $\Delta$ 35 may play a role in the process of cell migration.

The role of Aip1/WDR1 during invasion is still unclear. To gain insight into a possible function related to invasiveness, invasion assays were performed. With MCF7 cells generally being uninvasive to mildly invasive, and Hs578T cells being highly-invasive, it was possible to examine the effects of WDR1 and WDR $\Delta$ 35 overexpression in cells with different predispositions to invasiveness. MCF7 cells transiently expressing GFP-WDR1 or GFP-WDR $\Delta$ 35 did not exhibit increased invasive capabilities compared to either control, and were not significantly different from each other (Figure 3.7). As expected, all Hs578T lines were more invasive than all MCF7 lines. However, despite Hs578T GFP-WDR1 and GFP-WDR $\Delta$ 35 cell lines showing lower invasiveness than the untransfected control, they did not show any significant differences from the GFP control cells. Overall, these invasion assays demonstrated that WDR1 or WDR $\Delta$ 35 does not have an overall effect on the invasive property of cancer cells with inherently different invasive qualities, at least when cells were transiently transfected. This suggested that both WDR1 isoforms are likely not involved or play a minor role in the invasion and migration process, although further studies are necessary to examine these properties.

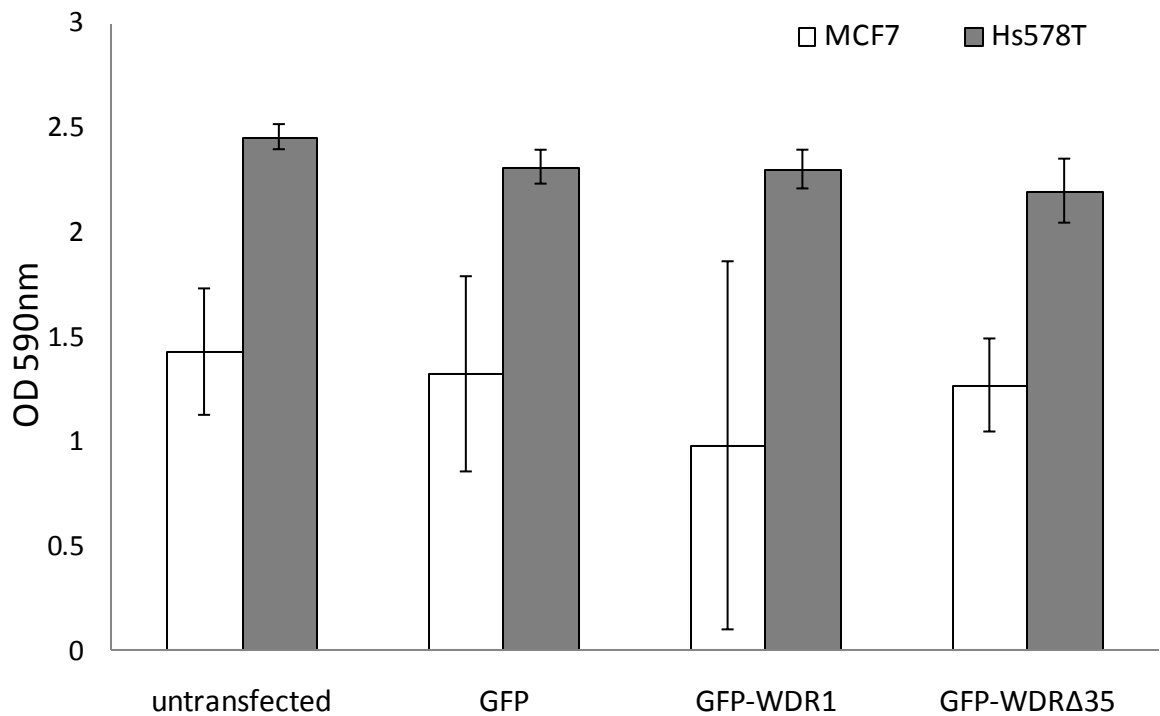


**Figure 3.7: Transient overexpression of WDR1 or WDRΔ35 does not significantly affect MCF7 or Hs578T invasiveness.** MCF7 and Hs578T cell lines expressing GFP-fusion proteins were serum-starved for approximately 3hr, and a suspension of approximately  $7 \times 10^7$  cells/ml was plated onto polycarbonate basement membrane inserts. Medium containing appropriate serum and EGF concentrations stimulated migration of cells over 48hr. To quantify cells that successfully invaded through the basement membrane, the OD at 590nm was measured. For each sample in each trial, two OD<sub>590</sub> readings were taken, and the average was used. Invasiveness of cells expressing GFP-WDR1 or GFP-WDRΔ35 was compared to invasiveness of GFP control cells.

## **A regulatory relationship exists between WDR1, WDR $\Delta$ 35, and cofilin in Hek293 cells**

To elucidate the relationship between WDR1 isoforms and cofilin, it was essential to examine expression at transcriptional and translational levels. To study this relationship initially, Hek293 GFP-WDR1 and GFP-WDR $\Delta$ 35 cell lines were examined. Using qRT-PCR analysis, the log of the relative quantification value (logRQ) of gene expression was compared (Figure 3.8). For stable GFP, GFP-WDR1, and GFP-WDR $\Delta$ 35 cell lines, the doxycycline-induced sample was calibrated to the corresponding uninduced sample. For example, gene expression in GFP(+) cells was calibrated to expression in GFP(-) cells. Gene expression in cells overexpressing HA-tagged human cofilin (HA-cofilin) was also calibrated to GFP(-) cells. Remarkably, endogenous WDR $\Delta$ 35 transcription increased almost 3-fold when cofilin was constitutively overexpressed as an HA-fusion protein, while endogenous WDR1 transcription was not affected. However, doxycycline-induced expression of GFP-WDR $\Delta$ 35 had no effect on endogenous cofilin, but did cause a moderate decrease in endogenous WDR1 transcription. Induction of GFP-WDR1 expression did not exhibit a reciprocal effect on endogenous WDR $\Delta$ 35 transcription, but did cause a slight increase in endogenous cofilin transcription. In general, it was observed that cofilin affected WDR $\Delta$ 35, which in turn affected WDR1, and subsequently WDR1 affected cofilin. Together, these data are evidence for a possible transcriptional regulatory interaction between cofilin and both WDR1 isoforms.

In addition, through Western blot analysis and densitometry, the translational relationship was also observed between WDR1 isoforms and cofilin (Figure 3.9).

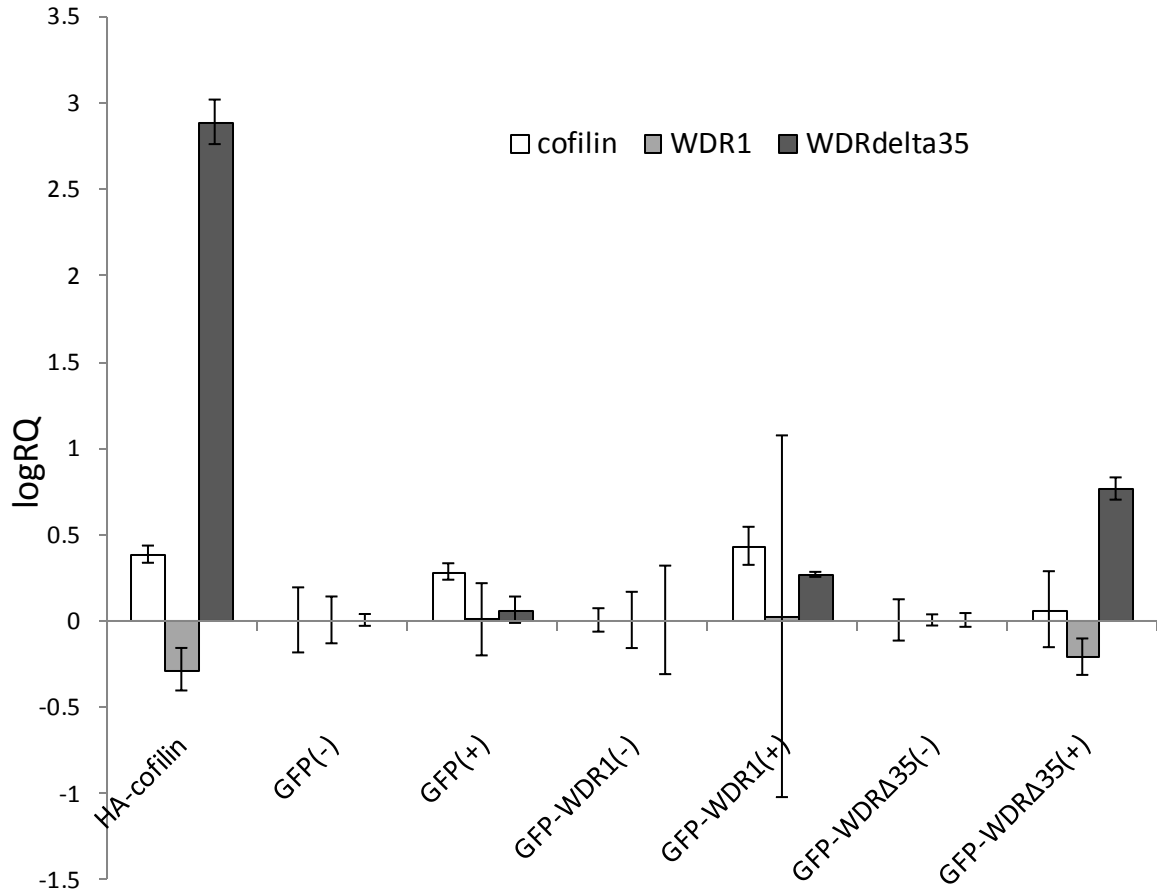
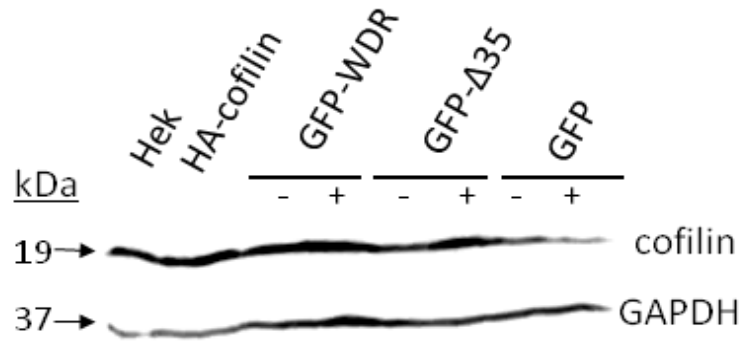


**Figure 3.8: In stable Hek293 cells, cofilin upregulates WDRΔ35 and WDRΔ35 downregulates WDR1 at the transcriptional level.** Total RNA was extracted from stable Hek293 cells containing GFP, GFP-WDR1, or GFP-WDRΔ35 after doxycycline-induced expression (+) or in the absence of doxycycline (-), and from cells transiently expressing HA-tagged cofilin (HA-cofilin). HA-cofilin was used as a positive control for cofilin expression. cDNA was then analyzed by qRT-PCR to detect cofilin, WDR1, and WDRΔ35 gene expression. Expression is represented by the log of the relative quantification value (logRQ). For each GFP cell line, the doxycycline-induced sample was calibrated to its corresponding uninduced sample. GAPDH was used as the endogenous control gene.

A



B

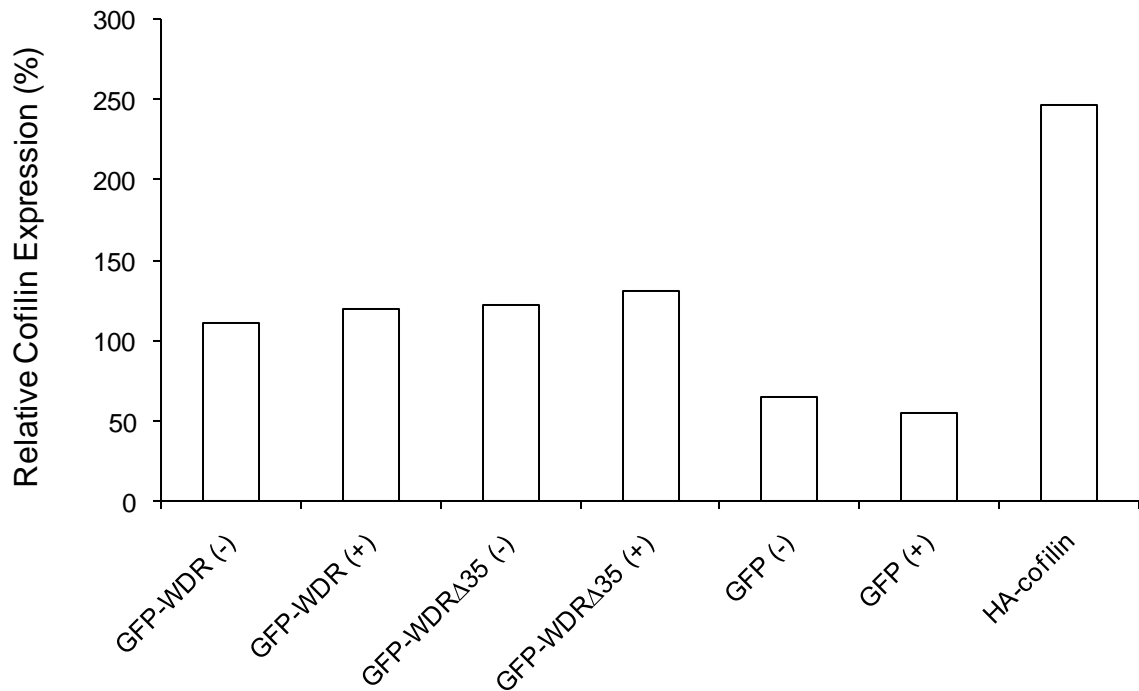


**Figure 3.9: In stable Hek293 cells, the affects of GFP-WDR1 or GFP-WDRΔ35 on cofilin translation are negligible.** (A) Western blotting detected cofilin expression in the presence (+) or absence (-) of doxycycline and (B) expression was quantified using densitometry. HA-cofilin expression was used as a positive control. Cofilin expression values were normalized to GAPDH to determine relative cofilin expression.

Densitometric values for cofilin were normalized to GAPDH to determine relative expression. In both cases, when exogenous WDR1 or WDR $\Delta$ 35 expression was induced by doxycycline, cofilin translation increased only slightly, but not significantly. Also, when comparing cofilin upregulation between cells stably expressing GFP-WDR1 and GFP-WDR $\Delta$ 35 expressing cells, levels in GFP-WDR $\Delta$ 35 cells were only slightly higher, suggesting that any effect WDR1 or WDR $\Delta$ 35 may have on cofilin translation is negligible.

### **WDR $\Delta$ 35 and cofilin may transcriptionally regulate each other in MCF7 cells**

To determine if the WDR1 isoform-cofilin relationship trends seen in Hek293 cell lines also exist in different breast cancer cell lines, gene expression analysis was conducted in MCF7 cells transiently transfected with GFP-WDR1 or GFP-WDR $\Delta$ 35 using qRT-PCR. It was important to quantify transcription levels of WDR1, WDR $\Delta$ 35, and cofilin in GFP-WDR1 and GFP-WDR $\Delta$ 35 cells compared to GFP control cells (Figure 3.10). In MCF7 cells, transient expression of GFP-WDR1 upregulated WDR $\Delta$ 35 transcription, but downregulated cofilin. Transient expression of GFP-WDR $\Delta$ 35 lead to an expected significant increase in WDR $\Delta$ 35 transcription and a downregulation of cofilin and WDR1. When cells were transiently transfected with HA-cofilin, endogenous WDR $\Delta$ 35 was upregulated to nearly the same expression levels seen during GFP-WDR $\Delta$ 35 expression, while WDR1 transcription levels remained unaffected. Therefore, these data suggest that WDR $\Delta$ 35 transcription levels are regulated by cofilin, and cofilin transcription may be influenced by WDR1 and WDR $\Delta$ 35. Furthermore, WDR1 expression may be controlled by WDR $\Delta$ 35 levels within the cell.



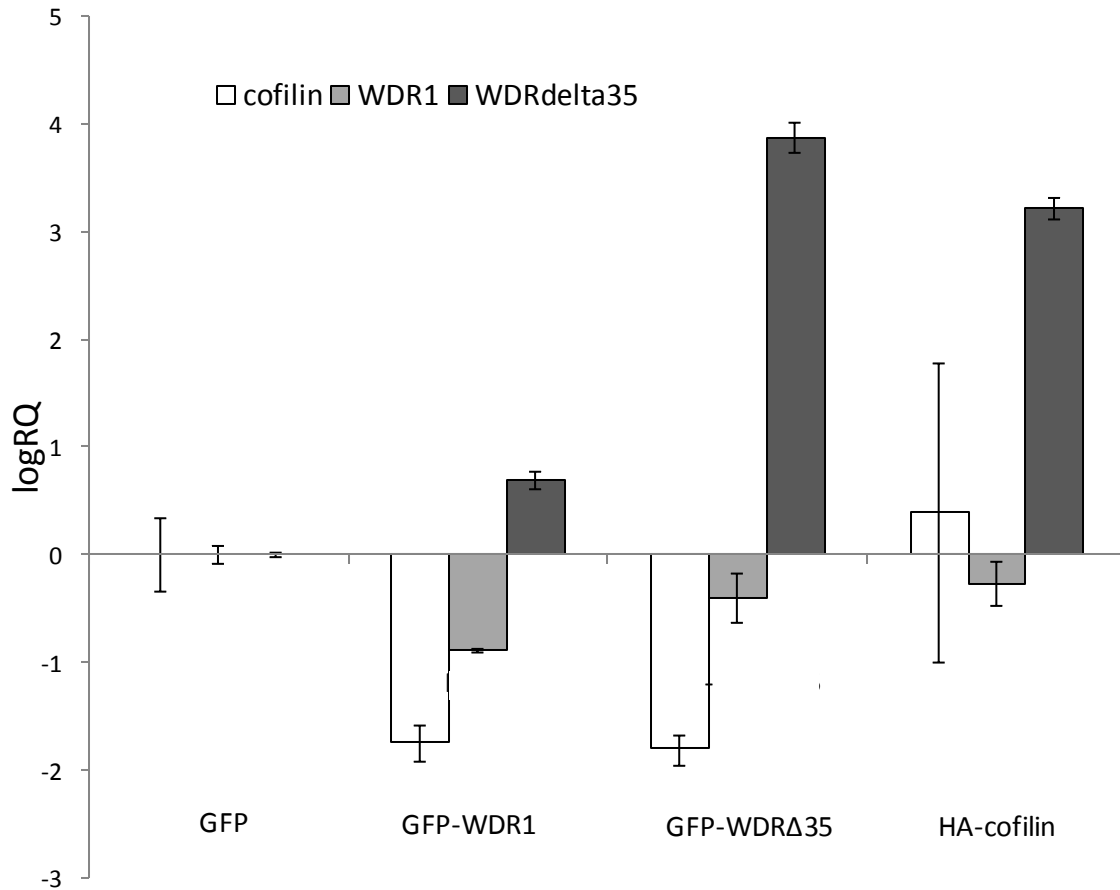


**Figure 3.10: In MCF7 cells, WDR1 and WDRΔ35 downregulate cofilin, and cofilin upregulates WDRΔ35.** Total RNA was extracted from MCF7 cells transiently expressing GFP, GFP-WDR1, GFP-WDRΔ35, or HA-cofilin. Gene expression analysis of cofilin, WDR1, and WDRΔ35 in each transient cell line was done using qRT-PCR. Expression of each gene is represented by the logRQ value. All samples were calibrated to GFP control cells, and GAPDH was used as the endogenous control gene.

### **Cofilin upregulates WDR $\Delta$ 35 and WDR1 downregulates WDR $\Delta$ 35 in Hs578T cells**

As with MCF7 cells, WDR1, WDR $\Delta$ 35, and cofilin expression levels were also quantified in transiently transfected Hs578T cell lines expressing GFP, GFP-WDR1, or WDR $\Delta$ 35 (Figure 3.11). In Hs578T cells, GFP-WDR1 expression downregulated WDR $\Delta$ 35 transcription, but did not change cofilin transcription levels. When cells expressed GFP-WDR $\Delta$ 35, WDR $\Delta$ 35 was predictably upregulated, while endogenous cofilin and WDR1 expression was not affected. When Hs578T cells were transiently transfected with HA-cofilin, there was a significant 3-fold increase in endogenous WDR $\Delta$ 35 transcription similar to the increase seen when GFP-WDR $\Delta$ 35 was transiently expressed. However, WDR1 transcription remained unaffected by HA-cofilin overexpression. Therefore, in Hs578T cells cofilin upregulates WDR $\Delta$ 35 transcription, while WDR1 downregulates it. Also, cofilin and WDR1 expression levels are not affected by each other or by WDR $\Delta$ 35 expression.

### **WDR1 and WDR $\Delta$ 35 transcription is not affected by brief activation of the EGF-cofilin pathway**

To further explore the relationship between both WDR1 isoforms and cofilin activation, MCF7 and Hs578T cell lines were subjected to EGF treatments at various time points. EGF is known to activate the cofilin pathway, therefore these treatments were necessary to see how stimulating this pathway affected WDR1 and WDR $\Delta$ 35. RNA was extracted from untreated cells (0sec) and from cells after 30sec, 1 min, 2 min, 5 min, and

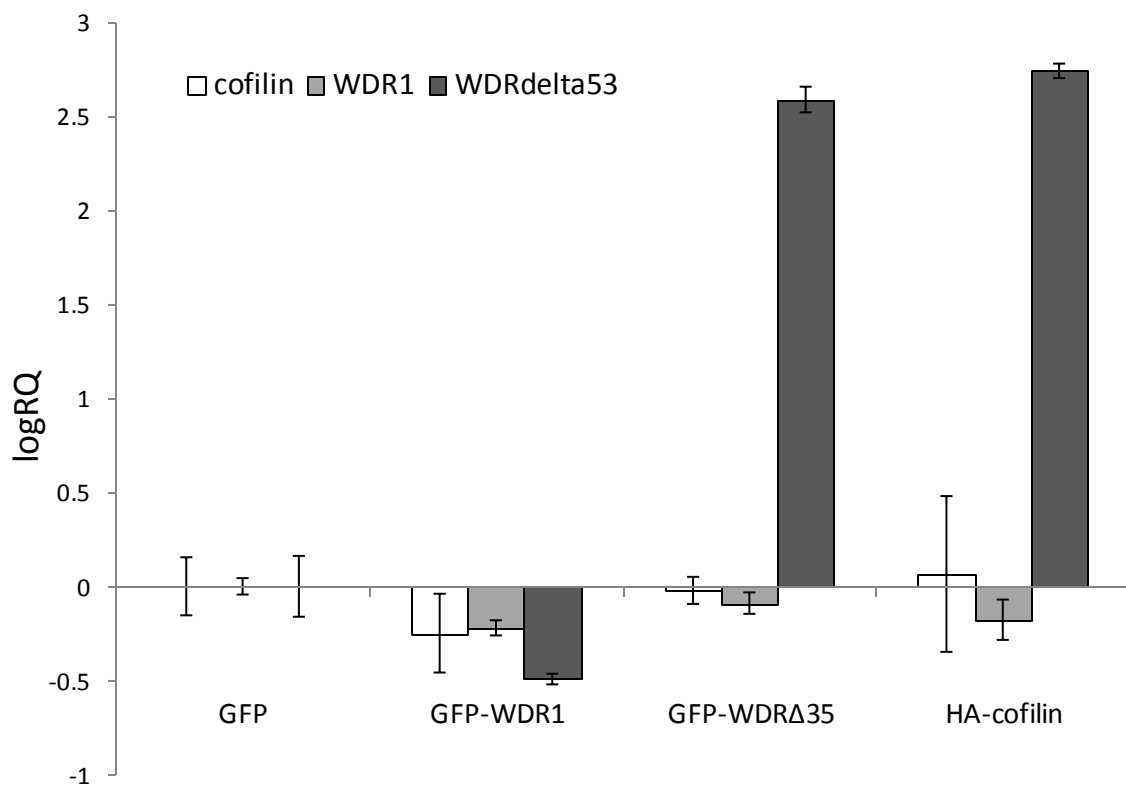


**Figure 3.11: In Hs578T cells, cofilin and WDR1 expression have opposite effects on WDRΔ35 transcription levels.** Total RNA was extracted from Hs578T cells transiently expressing GFP, GFP-WDR1, GFP-WDRΔ35, or HA-cofilin. Gene expression analysis of cofilin, WDR1, and WDRΔ35 in each transient cell line was done using qRT-PCR. Expression of each gene is represented by the logRQ value. All samples were calibrated to GFP control cells, and GAPDH was used as the endogenous control gene.

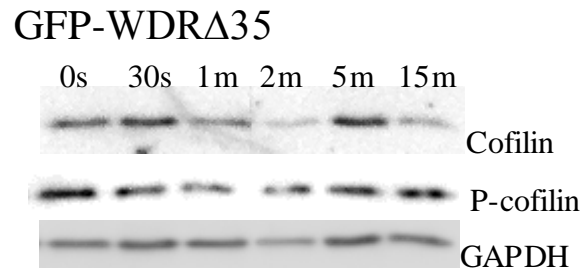
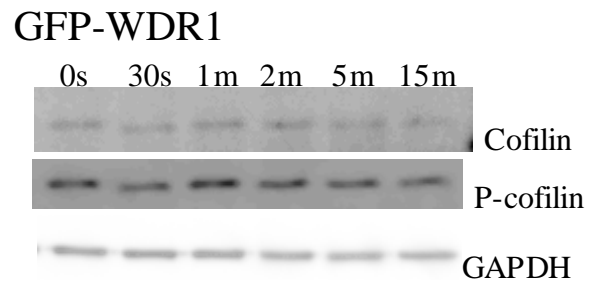
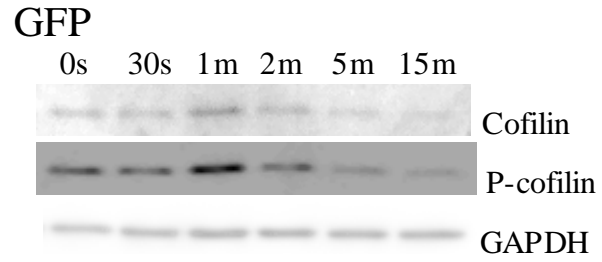
15min of EGF stimulation, then was converted to DNA for qRT-PCR analysis. To determine if WDR1 or WDR $\Delta$ 35 transcription could be influenced by cofilin, gene expression assays were performed on EGF-stimulated untransfected MCF7 or Hs578T cell lines (data not shown). Gene expression analysis was also done in EGF-treated MCF7 and Hs578T cells transiently expressing GFP, GFP-WDR1, or GFP-WDR $\Delta$ 35 (data not shown). Quantitative analysis revealed that there was no significant relationship between either of the WDR1 isoforms and cofilin activation at early time periods following EGF stimulation. Therefore, during the brief time course after EGF addition, WDR1 and WDR $\Delta$ 35 expression remained unchanged.

**In MCF7 cells, WDR1 protein expression stabilizes inactivation of cofilin, while WDR $\Delta$ 35 expression increases active cofilin levels**

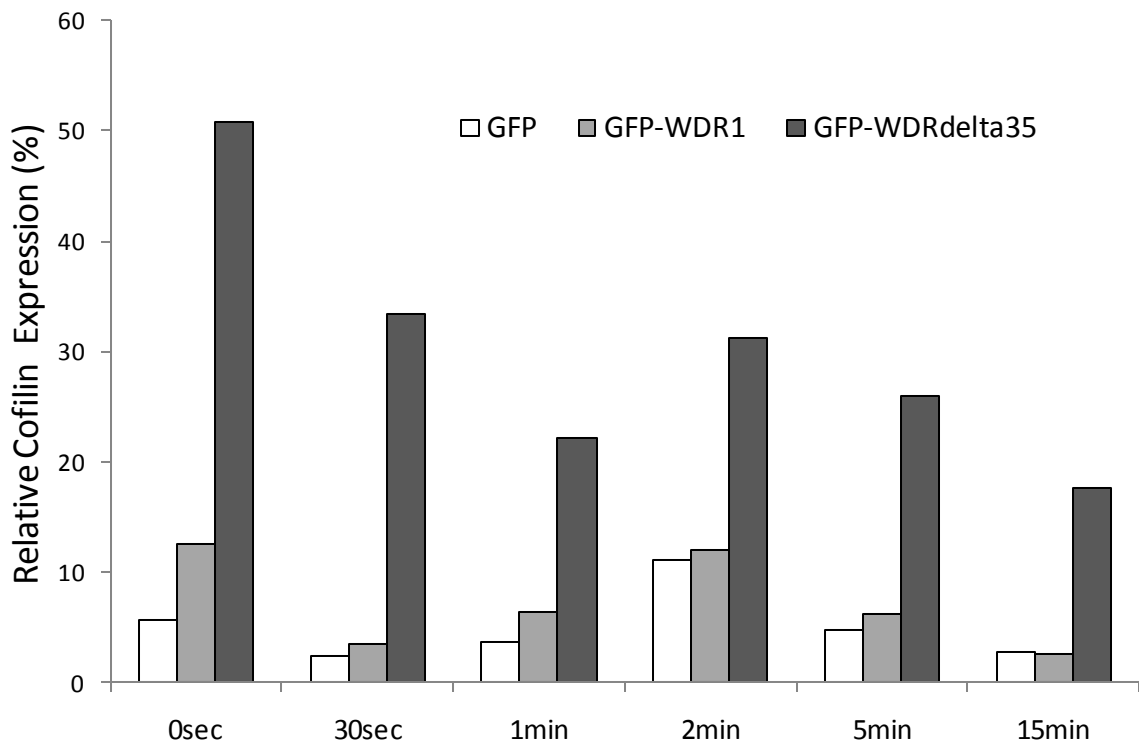
In order to study the role of WDR1 and WDR $\Delta$ 35 in cofilin activation, transiently transfected MCF7 cell lines were subjected to treatment with EGF to activate the cofilin regulatory pathway. Cofilin exists in the cell in two forms: dephosphorylated (active) and phosphorylated (inactive). To further uncover the details of a WDR1 isoform-cofilin relationship in terms of activation, it was necessary to analyze cofilin and phospho-cofilin protein expression in GFP-WDR1 and GFP-WDR $\Delta$ 35 cell lines using Western blots (Figures 3.12A), which were further analyzed using densitometry (Figure 3.12 B-C). All active and inactive cofilin expression levels at different time points were compared to unstimulated cells (0sec) as a negative control, and to cells transiently transfected with

**Figure 3.12: During induction of the cofilin regulation pathway in MCF7 cells, GFP-WDR1 stabilizes inactive cofilin, while GFP-WDR $\Delta$ 35 increases active cofilin.** MCF7 cells were transiently transfected with GFP, GFP-WDR1, or GFP-WDR $\Delta$ 35. Each cell line was serum-starved, then stimulated with 5ng/ml EGF for 30sec, 1min, 2min, 5min, and 15min. As a negative control, unstimulated cells (0sec) were used. HA-cofilin expression was used as a positive control (not shown). (A) Western blotting detected cofilin (active) and phospho-cofilin (inactive) expression in MCF7 cells transiently expressing GFP-fusion proteins. (B) Expression levels were quantified using densitometry. Active and inactive cofilin expression values were normalized to GAPDH expression to determine their relative expression in GFP, GFP-WDR1, and GFP-WDR $\Delta$ 35. Expression levels in GFP-WDR1 and GFP-WDR $\Delta$ 35-expressing cells were compared to GFP expression levels.

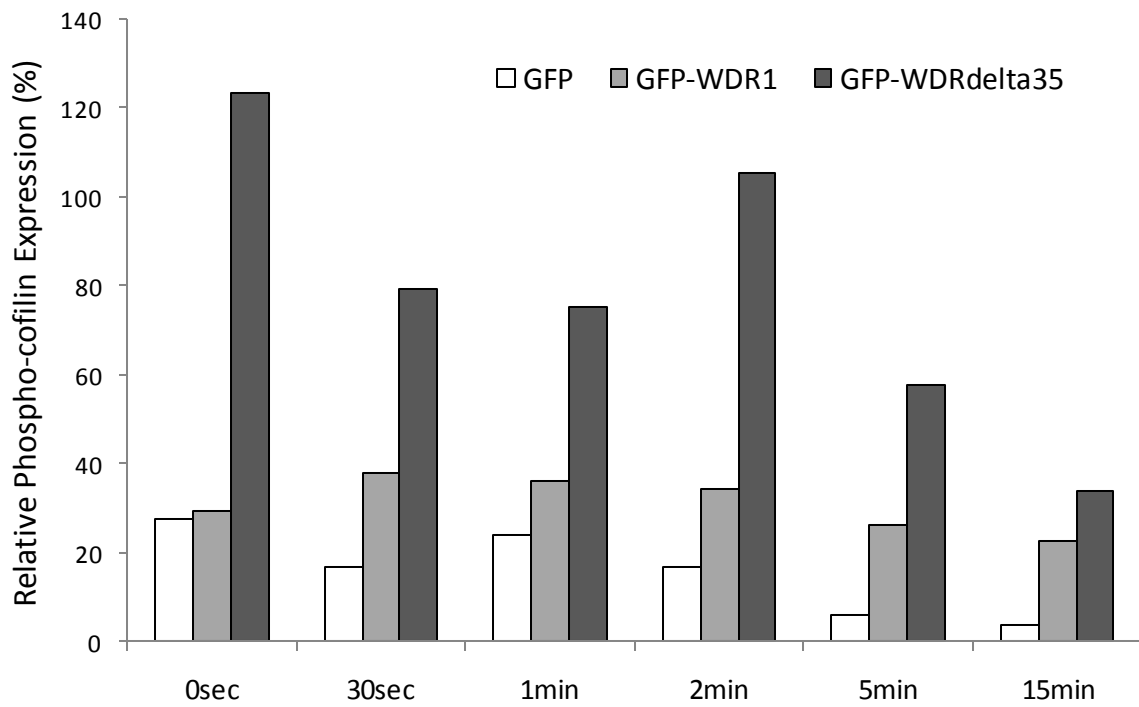
A



## B Cofilin



## C P-cofilin (inactive)



GFP to control for transfection. Therefore, any changes in active or inactive cofilin levels were attributed to transiently transfected GFP-WDR1 or GFP-WDR $\Delta$ 35 expression during EGF stimulation of the cofilin regulatory pathway. When cells transiently transfected with GFP-WDR1 were treated with EGF, inactivation of cofilin appeared to be maintained and increased moderately but not significantly over time compared to cells transfected with GFP. However, total cofilin expression levels were not affected significantly. In contrast, when the cofilin activation pathway was stimulated by EGF in cells expressing GFP-WDR $\Delta$ 35, total cofilin expression increased moderately. Inactive cofilin was again sustained and increased slightly compared to expression levels in GFP control cells. Overall, data suggested that WDR1 and WDR $\Delta$ 35 promoted the stabilization of inactive cofilin levels, however WDR $\Delta$ 35 also upregulated expression of total cofilin.

**In Hs578T cells, WDR1 protein expression stabilizes inactivation of cofilin, while WDR $\Delta$ 35 increases total cofilin**

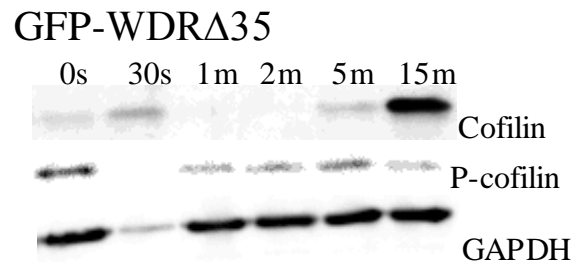
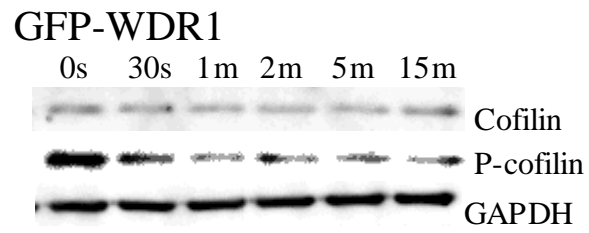
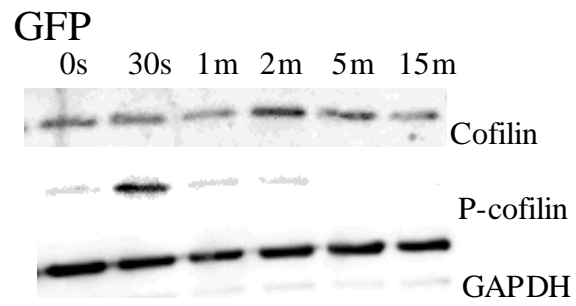
The effect of WDR1 and WDR $\Delta$ 35 expression on cofilin activity in EGF-stimulated Hs578T cells transiently transfected with GFP-fusion proteins was also studied. It was necessary to investigate cofilin and phospho-cofilin protein expression in GFP-WDR1 and GFP-WDR $\Delta$ 35 cell lines using Western blots (Figure 3.13A), followed by quantification of expression using densitometry (Figures 3.13B-C). All active and inactive cofilin expression levels at different time points were compared to unstimulated cells (0sec) as a negative control, and to cells transiently transfected with GFP to control



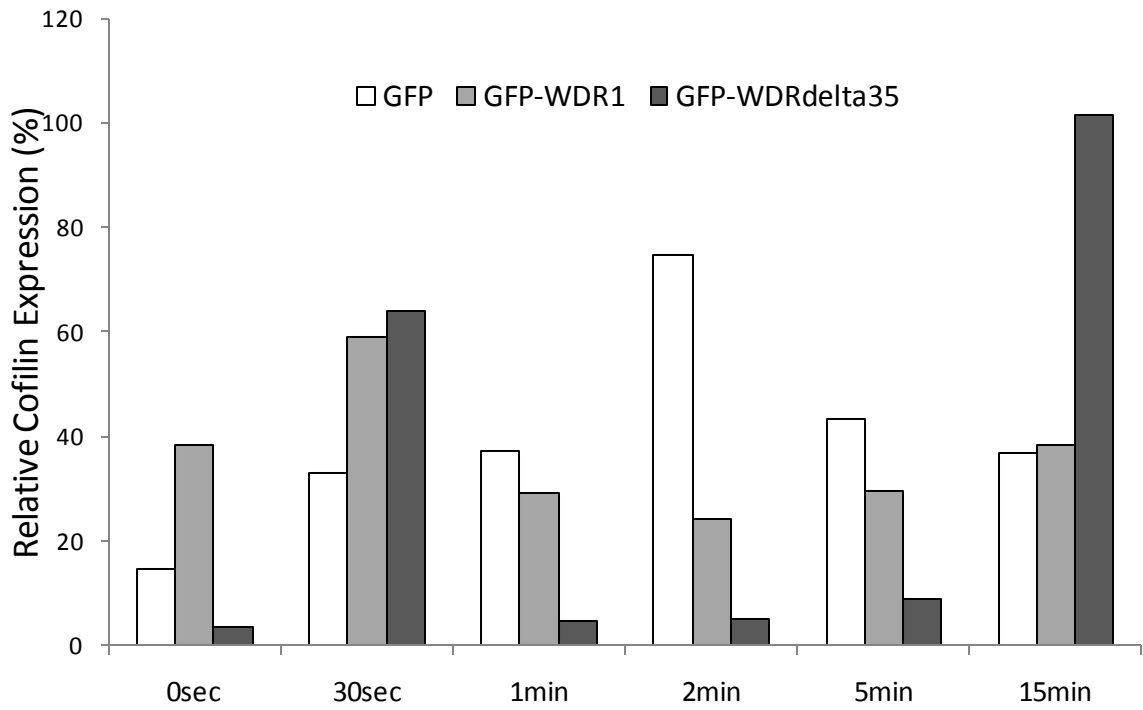
**Figure 3.13: During induction of the cofilin regulation pathway in Hs578T cells, GFP-WDR1 stabilizes inactive cofilin, while GFP-WDR $\Delta$ 35 increases active cofilin.**

Hs578T cells were transiently transfected with GFP, GFP-WDR1, or GFP-WDR $\Delta$ 35. Each cell line was serum-starved, then stimulated with 10ng/ml EGF for 30sec, 1min, 2min, 5min, and 15min. As a negative control, unstimulated cells (0sec) were used. HA-cofilin expression was used as a positive control (not shown). (A) Western blotting detected cofilin (active) and phospho-cofilin (inactive) expression in Hs578T cells transiently expressing GFP-fusion proteins. (B) Expression levels were quantified using densitometry. Active and inactive cofilin expression values were normalized to GAPDH expression to determine their relative expression in GFP, GFP-WDR1, and GFP-WDR $\Delta$ 35. Expression levels in GFP-WDR1 and GFP-WDR $\Delta$ 35-expressing cells were compared to GFP expression levels.

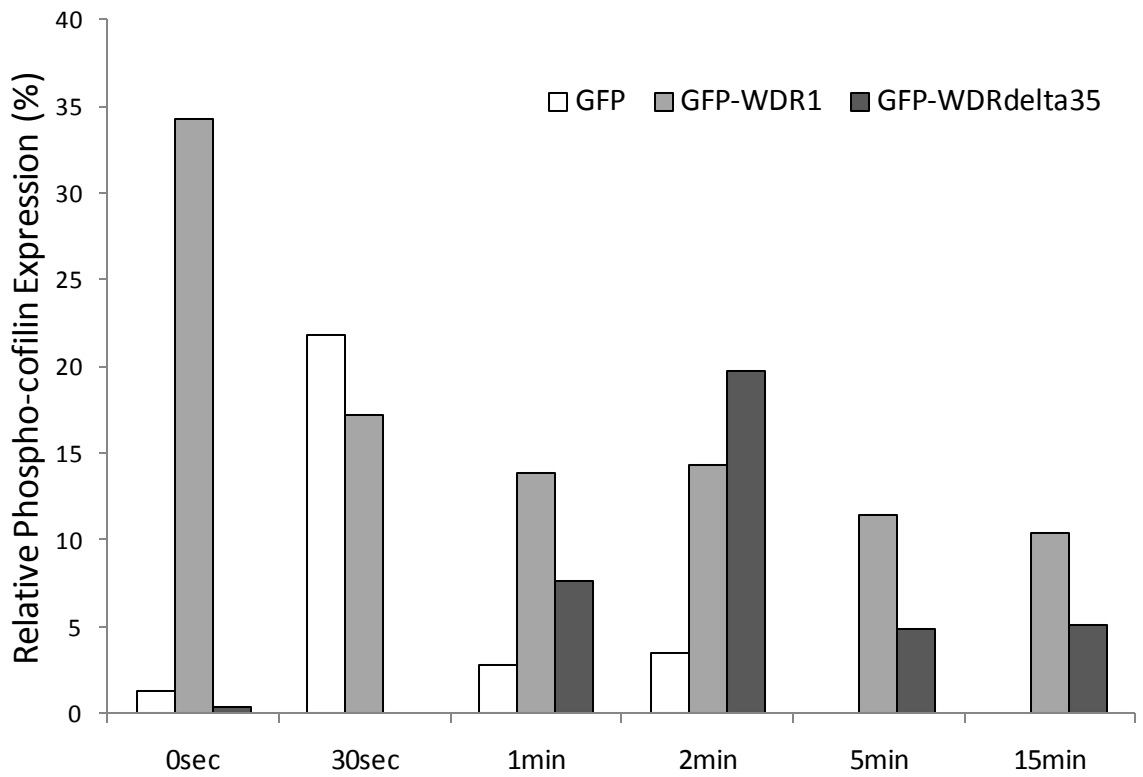
A



## B Cofilin



## C P-cofilin (inactive)



for transfection. When the cofilin activation pathway was stimulated by EGF in cells transiently expressing GFP-WDR1 or GFP-WDR $\Delta$ 35, inactivation of cofilin was downregulated after EGF stimulation, but was maintained compared to GFP control cells. Quantification of total cofilin expression in Hs578T cells transiently transfected with GFP-WDR $\Delta$ 35 showed that cofilin levels increased moderately after 15min of EGF stimulation. In summary these data indicated that WDR1 and WDR $\Delta$ 35 promoted the stabilization of inactive cofilin levels, while WDR $\Delta$ 35 also increased expression of cofilin.

When data from MCF7 and Hs578T protein expression studies are taken together, results suggest that in different types of breast cancer cell lines, there is an intimate regulatory network set up between cofilin activation/inactivation and the amount of WDR1 and WDR $\Delta$ 35 present within the cell. Further studies are required in order to fully understand these interactions and their significance.

## Chapter Four: Discussion

Despite plenty of evidence to support the existence of an Aip1 homolog in higher eukaryotes called WDR1, little has been confirmed about its function, expression, and regulation in mammals. There is a lack of information regarding WDR1's relationship with cofilin, as well as the functional characterization of WDR1's truncated isoform, WDR $\Delta$ 35. Results from this study provide evidence that WDR1 and WDR $\Delta$ 35 both participate in the regulation of cofilin activity in different ways.

As mentioned previously, WDR $\Delta$ 35 has 419bp of the cDNA sequence removed, from 421-840 nucleotide bases (Noone and Hubberstey, unpublished). This excised section represents exons three, four, and five. Extensive studies on Aip1/WDR1 in *C. elegans* revealed that five residues are responsible for its association with cofilin-bound actin and its ability to promote disassembly: E126, D168, K181, F182, and F192 (Mohri *et al.*, 2004). These specific residues are conserved between *C. elegans* Aip1 and human WDR1. Interestingly, splicing of WDR $\Delta$ 35 removes all of these amino acids, except for F192 (Figure 4.1). Continued mutational studies of Aip1 by Mohri *et al.* (2006) demonstrated that a single point mutation of any one of the residues in question failed to fully disrupt Aip1 activity. Single mutations also did not hinder the rescue of null Aip1 phenotypes. Most importantly, collective mutation of four of the five Aip1 residues entirely abrogated actin disassembly and the ability to rescue null phenotypes. As WDR $\Delta$ 35 splicing removes these residues in such a way that mimics the simultaneous mutations performed by Mohri *et al.* (2006), it is likely that the truncated isoform may also lack actin binding

WDR1	MPYEIKKVFASLPQVERGVSKIIGGDPKGNFLYTNKGCVILRNIDNPALADIYTEHAHQ	60
WDRΔ35	MPYEIKKVFASLPQVERGVSKIIGGDPKGNFLYTNKGCVILRNID-----	46
WDR1	VVVAKYAPSGFYIASGDVSGKLRIWDTTQKEHLLKYEYQPFAGKIKDIAWTEDSKRIAVV	120
WDRΔ35	-----	
WDR1	GEGREKFGAVFLWDSGSSVGEITGHNKVINSVDIKQSRPYRLATGSDDNCAAFFEGPPFK	180
WDRΔ35	-----	
WDR1	FKFTIGDHSRFFVNCVRFSPDGNRFATASADGQIYIYDGKTGEKVCALGGSKAHDGGIYAI	240
WDRΔ35	-----DHSRFFVNCVRFSPDGNRFATASADGQIYIYDGKTGEKVCALGGSKAHDGGIYAI	100
WDR1	SWSPDSTHLLSASGDKTSKIWDVSVNSVSVSTFPMGSTVLDQQLGCLWQKDHLLSVLSLGY	300
WDRΔ35	SWSPDSTHLLSASGDKTSKIWDVSVNSVSVSTFPMGSTVLDQQLGCLWQKDHLLSVLSLGY	160
WDR1	INYLDRNNPSKPLHVIKGHSKSIQCLTVHKNGGKSYIYSGSHDGHINYWDSETGENDSFA	360
WDRΔ35	INYLDRNNPSKPLHVIKGHSKSIQCLTVHKNGGKSYIYSGSHDGHINYWDSETGENDSFA	220
WDR1	GKGHTNQVSRMTVDESGQLISCSMDDTVRYTSLMLRDYSGQGVVKLDVQPKCVAVGPGGY	420
WDRΔ35	GKGHTNQVSRMTVDESGQLISCSMDDTVRYTSLMLRDYSGQGVVKLDVQPKCVAVGPGGY	280
WDR1	AVVVCIGQIVLLKDQRKCFSIDNPGYEPEVVAVHPGGDTVAIGGVDGNVRLYSILGTTLK	480
WDRΔ35	AVVVCIGQIVLLKDQRKCFSIDNPGYEPEVVAVHPGGDTVAIGGVDGNVRLYSILGTTLK	340
WDR1	DEGKLLLEAKGPVTDVAYSHDGAFLAVCDASKVVTVFVSADGYSENNVFYGHAKIVCLAW	540
WDRΔ35	DEGKLLLEAKGPVTDVAYSHDGAFLAVCDASKVVTVFVSADGYSENNVFYGHAKIVCLAW	400
WDR1	SPDNEHFASGGMDMMVYVWTLSDPETRVKIQDAHRLHHVSSLAWLDEHTLVTTSHDASVK	600
WDRΔ35	SPDNEHFASGGMDMMVYVWTLSDPETRVKIQDAHRLHHVSSLAWLDEHTLVTTSHDASVK	460
WDR1	EWTITY	606
WDRΔ35	EWTITY	466

**Figure 4.1: Human WDR1 and WDRΔ35 protein sequence alignment and proposed functional residues.** This ClustalW alignment illustrates the location of the amino acids demonstrated by Mohri *et al.* (2004; 2006) to be responsible for actin binding activity of Aip1/WDR1. Functional residues are highlighted in red. Dashed lines represent the section removed from WDRΔ35 due to splicing of exons three, four, and five.

and disassembly-enhancing abilities. These observations defend a role for WDRΔ35 that is entirely different from that of WDR1. However, alternative splicing does not remove

any of the kelch-like motifs found in WDR1 (Noone and Hubberstey, unpublished), implying that WDR $\Delta$ 35's role is likely also one involving protein-protein interactions.

Other data support the theory that the WDR1 isoforms may have similar functions, but in different cell types. RT-PCR analysis has shown that WDR1 isoforms are differentially expressed in a tissue-specific manner. WDR $\Delta$ 35 was the only isoform expressed in cardiac and skeletal muscle tissues (Noone and Hubberstey, unpublished). Quantitative RT-PCR expression analysis indicated that WDR1 was in fact expressed in these two tissues, but at significantly lower levels than WDR $\Delta$ 35. These transcription levels were also much lower than WDR1 and WDR $\Delta$ 35 expression levels seen in other tissues, including brain, breast, lung, and testis (Correa and Hubberstey, unpublished data). In these same two tissue types (cardiac and skeletal muscle), cofilin-2 is the only cofilin isoform being expressed (Ono *et al.*, 1994; van Troys *et al.*, 2008). It is possible that WDR1 evolved in higher eukaryotes in parallel to cofilin's tissue-specific expression.

In addition to differential expression in normal tissues, Correa and Hubberstey (unpublished data) showed that when gene expression analysis of WDR1 and WDR $\Delta$ 35 was done using qRT-PCR analysis in various breast cancer lines, including Hs578T cells, WDR $\Delta$ 35 transcription levels were always higher than WDR1 levels. However, expression levels of both genes were notably higher in normal human breast tissue than in any of the breast cancer cell lines.

The first aim of this study was to determine if mammalian WDR1 and/or WDR $\Delta$ 35 are involved in cell migration and invasion processes. Although a great deal of evidence has confirmed a role for Aip1/WDR1 during cell migration and a likely role during invasion, WDR $\Delta$ 35's influence on these processes is completely unknown. One

study showed that overexpressing Aip1 in *Dictyostelium* rescued migration defects in null-mutants, suggesting that Aip1 promotes cell motility (Konzok *et al.*, 1999). Several different studies employing overexpression of GFP-tagged Aip1/WDR1 to examine localization patterns during migration revealed that Aip1/WDR1 associated with actin networks in membrane protrusions (Tsuji *et al.*, 2009), and that WDR1 was generally localized to the leading edge of migrating fibroblasts (Noone and Hubberstey, unpublished). Another study showed that when murine neutrophils experienced a partial loss of WDR1 function, cell migration rates decreased and F-actin accumulated (Kile *et al.*, 2007). Also, Kato *et al.* (2008) demonstrated that mammalian WDR1 plays a critical role in the directional migration of Jurkat T-lymphoma cells by enhancing cofilin activity during membrane protrusion formation.

Despite this evidence supporting a role for WDR1 in cell motility, wound-healing and invasion assays in this study indicated that WDR1 or WDR $\Delta$ 35 did not affect overall migration rate or the invasiveness of MCF7 or Hs578T cells (Figure 3.6 and Figure 3.7). However, confocal imaging revealed that cells expressing GFP-tagged WDR $\Delta$ 35 migrated into the wound more efficiently than surrounding untransfected cells. MCF7 cells overexpressing GFP-WDR1 showed a decrease in migration rate, while overexpressing Hs578T cells showed an increase. Since only 30% of MCF7 or Hs578T cells overexpressed WDR1 or WDR $\Delta$ 35, it may explain why overall migration rates on the plates remained unaffected. If GFP-WDR $\Delta$ 35 was more highly expressed, the observed movement of overexpressing cells into the wound would likely have been corroborated with an increase in migration rate. It is likely that expression of GFP-WDR $\Delta$ 35 in these cells did promote migration, but did not make a significant impact on



overall migration rate since 70% of cells remained untransfected and therefore exhibited normal WDR $\Delta$ 35 expression levels. Furthermore, GFP-fusion protein overexpression itself was transient, and although our other observations confirmed prolonged expression (Figure 3.4), cell proliferation during wound closure would increase the number of non-expressing cells, especially if proliferation was inhibited by WDR $\Delta$ 35 in overexpressing cells. Overall WDR1 and WDR $\Delta$ 35 may be involved in cell motility, however more research is necessary to confirm these findings.

The second aim of this research was to understand the regulatory and activation relationships between WDR1 and WDR $\Delta$ 35 and cofilin. Other research groups have alluded to the fact that information regarding Aip1/WDR1 regulation is lacking (Mohri *et al.*, 2006; Clark and Amberg, 2007). To determine the regulatory relationship of WDR1 and WDR $\Delta$ 35 with cofilin and each other, it was necessary to examine transcriptional expression. In stable TREX cell lines (Figure 3.8) and transient MCF7 (Figure 3.10) and Hs578T (Figure 3.11) breast cancer cell lines, the major result was that an increase in cofilin significantly upregulated WDR $\Delta$ 35 transcription. Also, in the stable TREX and transient MCF7 cell lines, upregulation of WDR $\Delta$ 35 caused a slight but significant downregulation of WDR1 transcription. In conclusion, these transcriptional studies indicate that WDR1 and WDR $\Delta$ 35 exhibit differences in expression and regulation. It is unclear exactly how cofilin or these WDR1 isoforms are involved in transcriptional regulation or what other factors may be involved. Other studies have indicated that cofilin contains a nuclear localization signal and that it is distributed in the nucleus (Nishida *et al.*, 1987; Okada *et al.*, 1999). Since our results indicate that cofilin clearly regulates WDR $\Delta$ 35 in all cases, it is possible that cofilin aids in the regulation of transcriptional

machinery. Many other proteins containing WD40 repeat motifs have been shown to be involved in RNA synthesis, processing, and chromatin assembly. Studies have demonstrated that these WD repeats are located on some transcription factor subunits and associated factors (Yamamoto and Horikoshi, 1997; Roberts, 2000; Li and Roberts, 2001). Although WDR1 has been characterized as a cytoplasmic protein, Okada *et al.* (1999) demonstrated that *Xenopus* Aip1/WDR1 is found in nuclei, and actually colocalizes with nuclear cofilin. WDR1, WDR $\Delta$ 35, and cofilin may also act within a signal transduction cascade that promotes transcriptional control of one another. Thus, transcriptional regulation would depend on WDR1, WDR $\Delta$ 35, and/or cofilin protein levels within the cytoplasm.

One problem to note during these transcriptional studies involves the overexpression of WDR1. It was very clear that each time WDR1 was overexpressed in MCF7 or Hs578T cells, total WDR1 transcription levels were decreased. If WDR1 was being successfully overexpressed in a cell line, transcription should have been significantly upregulated. It is unclear why this result was obtained repeatedly. All GFP-tagged WDR1 expressing cells exhibited expression levels comparable to those seen in GFP-WDR $\Delta$ 35 cells. There were likely no technical issues with qRT-PCR, as upregulation of WDR1 transcription could be demonstrated in other cells (data not shown). Thus the WDR1 primer-probe set was functional.

In the literature, an overwhelming amount of data support Aip1/WDR1 as an enhancer of cofilin activity (Okada *et al.*, 1999; Rodal *et al.*, 1999; Mohri *et al.*, 2004; Mohri *et al.*, 2006; Clark *et al.*, 2006; Clark and Amberg, 2007), but no information is available to explain how WDR1 isoforms actually affect the activation or translation of

cofilin. Clark and Amberg (2007) suggest that Aip1/WDR1-enhanced, cofilin-mediated actin turnover is likely dependent upon Aip1/WDR1 and cofilin protein concentrations. They also propose that this mode of actin turnover may be moderated by other regulatory proteins or even by other actin-interacting proteins. Therefore, in addition to examining transcriptional relationships, it was essential to assess the relationship between both WDR1 isoforms and cofilin activation status at the protein level in order to determine whether or not WDR1 and WDR $\Delta$ 35 were a part of the EGF-regulated signal transduction cascade that controls cofilin activity. The affects of overexpressing WDR1 or WDR $\Delta$ 35 on the activation status were examined by quantifying both cofilin and phospho-cofilin expression in MCF7 and Hs578T cells (Figure 3.12 and Figure 3.13). Our results suggest that expression of WDR $\Delta$ 35 during EGF stimulation promotes cofilin activation by upregulating total protein expression, while WDR1 regulates cofilin activity by stabilizing inactivation/phosphorylation of cofilin.

In short, the amounts of WDR1 and WDR $\Delta$ 35 expressed within the cell can closely regulate cofilin's activation status. Clark and Amberg (2007) further suggest that regulation of Aip1/WDR1 and cofilin concentrations within the cell may dictate whether actin filaments are severed, polymerized, or capped at the barbed end. It has been shown that cofilin concentration can in fact regulate its own activity. Cofilin-mediated filament severing tends to occur at lower concentrations, while increased cofilin levels promote its actin-assembling abilities (Andrianantoandro and Pollard, 2006; van Troys *et al.*, 2008). Taking this into account along with our results, it is possible that WDR1 expression levels regulate cofilin-mediated F-actin severing versus polymerization since it regulates the inactivation levels of cofilin.

As for WDR $\Delta$ 35, how and why it may upregulate cofilin expression and/or activation remains unclear. An extensive study by van Rheenen *et al.* (2007) elucidated a model for EGF-regulated cofilin activity involving LIMK phosphorylation mechanisms as well as PIP<sub>2</sub>-cofilin binding working as one regulatory system. To summarize their model, EGF-induced PIP<sub>2</sub> reduction releases cofilin from the plasma membrane. Cofilin then severs and disassembles F-actin, remaining bound to the resulting depolymerized actin monomers. LIMK phosphorylates cofilin to release it from the actin monomer, and SSH subsequently dephosphorylates cofilin. Active, or dephosphorylated, cofilin can then bind again either to PIP<sub>2</sub> to be sequestered, or to another actin filament for further depolymerization. Structurally, WDR $\Delta$ 35 retains the residues predicted to be responsible for its binding to cofilin (Mohri *et al.*, 2004; Clark *et al.*, 2006; Mohri *et al.*, 2006; Clark and Amberg, 2007). Based on this information, WDR $\Delta$ 35 could increase cofilin expression and/or activation in order to promote cofilin-G-actin association and/or to enhance cofilin's reassociation with F-actin or PIP<sub>2</sub>. Despite any speculation, more information is required to accurately identify how WDR1 and WDR $\Delta$ 35 regulate cofilin expression and activation.

## Chapter 5: Conclusions

In summary, this research demonstrates that cofilin transcription can promote upregulation of WDR $\Delta$ 35 transcription. Also, during EGF induction, WDR1 expression stabilizes cofilin inactivation, while WDR $\Delta$ 35 promotes cofilin expression and/or activation. In addition, this study reveals that WDR1 may play a role during cancer cell migration and invasion, and is the first to provide evidence of the role of WDR $\Delta$ 35 in these processes. Overall this study indicates that WDR1 isoforms are functionally distinct. Further research is required to fully understand how and why regulation of WDR1 and WDR $\Delta$ 35 and their effects on cell motility and cofilin activity differ.

More information is required to fully understand the differences in WDR1 isoforms suggested here. Using a more specific WDR1 antibody that targets an area within exons 3-5, and developing a WDR $\Delta$ 35-specific antibody raised against the exon 2-6 junction would enable further translational studies. Western blotting to detect WDR1 and WDR $\Delta$ 35 protein expression would then fully coincide with transcriptional studies. Examining transcriptional expression and regulatory relationships between WDR1 isoforms and cofilin in other breast cancer cell lines and in normal breast tissue may also provide a more comprehensive analysis. Specifically, this could be done in the Hs578Bst cell line, which is the normal breast cell line derived from the same patient as Hs578T tumour cells. Despite the research presented here, continued studies to characterize the differences between WDR1 isoforms will be essential. Employing the cap-dependent RACE (Rapid Amplification of cDNA Ends) technique would be useful for determining whether WDR1 and WDR $\Delta$ 35 are products of different transcription start sites or of alternative splicing.

Also, to complement the research presented in this study, it will be critical to examine the effects of silencing WDR1 isoforms on cell motility and regulatory interactions with cofilin. Applying RNA interference techniques to create WDR1 and WDR $\Delta$ 35 knock-downs will further illustrate the involvement and necessity of WDR1 isoforms in various cellular processes. In addition, repeating many of these experiments using stable GFP-fusion protein cell lines would corroborate the data analyzed for the research discussed here, in which cell lines transiently expressing GFP-fusion proteins were utilized. Finally, conducting further long-term live-cell imaging during unstimulated and EGF-stimulated wound-healing assays would provide a clearer analysis of cell migration over an extended period of time. Individual cells expressing GFP-WDR1 or GFP-WDR $\Delta$ 35 could then be monitored constantly.

Overall, understanding the underlying mechanisms that allow for cancer cells to migrate and become invasive is critical. To further define whether WDR1 isoforms are an essential part of these mechanisms or not and how they are regulated, research in this area must be continued. Since invasion and subsequent metastasis are the distinguishing characteristics of malignant tumor cells, learning how to inhibit these acquired traits is an important step in metastatic cancer prevention.

## References

Adler, HJ, Sanovich, E, Brittan-Powell, EF, Yan, K, and Dooling, RJ. (2008) WDR1 presence in songbird basilar papilla. *Hear Res.* 240(1-2): 102-111.

Adler, HJ, Winnicki, RS, Gong, TW, and Lomax, MI. (1999) A gene upregulated in the acoustically damaged chick basilar papilla encodes a novel WD40 repeat protein. *Genomics.* 56(1): 59-69.

- Alberts, B, Johnson, A, Lewis, J, Raff, M, Roberts, K, and Walter, P. (2008) *Molecular Biology of the Cell*. 5<sup>th</sup> Ed.
- Amano, T, Tanabe, K, Eto, T, Narumiya, S, and Mizuno, K. (2001) LIM-kinase 2 induces formation of stress fibres, focal adhesions and membrane blebs, dependent on its activation by Rho-associated kinase-catalyzed phosphorylation at threonine-505. *Biochem J*. 354: 149–159.
- Amberg, DC, Basart, E, and Botstein, D. (1995) Defining protein interactions with yeast actin *in vivo*. *Nat Struct Biol*. 2(1): 28-35.
- Andrianantoandro, E, and Pollard, T. (2006) Mechanism of actin filament turnover by severing and nucleation at different concentrations of ADF/cofilin. *Mol Cell*. 24: 13-23.
- Bacus, SS, Kiguchi, K, Chin, D, King, CR, and Huberman E. (1990) Differentiation of cultured human breast cancer cells (AU-565 and MCF-7) associated with loss of cell surface HER-2/neu antigen. *Mol Carcinog*. 3: 350-362.
- Balcer, HI, Goodman, AL, Rodal, AA, Smith, E, Kugler, J, Heuser, JE, and Goode, BL. (2003) Coordinated regulation of actin filament turnover by a high-molecular-weight Srv2/CAP complex, cofilin, profilin, and Aip1. *Curr Biol*. 13: 2159-2169.
- Bamburg, JR, Harris, HE, and Weeds, AG. (1980) Partial purification and characterization of an actin depolymerising factor from brain. *FEBS Lett*. 121: 178–182.
- Bamburg, JR, and Wiggans, OP. (2002) ADF/cofilin and actin dynamics in disease. *Trends Cell Biol*. 12: 598-605.
- Barber, MA, and Welch, HCE. (2006) PI3K and RAC signalling in leukocyte and cancer cell migration. *Bull Cancer*. 93(5): E44-52.
- Brooks, SC, Locke, ER, and Soule, HD. (1973) Estrogen receptor in a human cell line (MCF-7) from breast carcinoma. *J Biol Chem*. 248(17): 6251-6253.
- Carrier, MF, Laurent, V, Santolini, J, Melki, R, Didry, D, Xia, GX, Hong, Y, Chua, NH, and Pantaloni, D. (1997) Actin depolymerizing factor (ADF/cofilin) enhances the rate of filament turnover: implication in actin-based motility. *J Cell Biol*. 136: 1307–1322.
- Clark, MG, Teply, J, Haarer, BK, Viggiano, SC, Sept, D, and Amberg, DC. (2006) A genetic dissection of Aip1p's interactions leads to a model for Aip1p-cofilin cooperative activities. *Mol Biol Cell*. 17: 1971-1984.

- Clark, MG, and Amberg, DC. (2007) Biochemical and genetic analyses provide insight into the structural and mechanistic properties of actin filament disassembly by the Aip1p-cofilin complex in *Saccharomyces cerevisiae*. *Genetics*. 176: 1527-1539.
- Condeelis, J, Singer, RH, and Segall, JE. (2005) The great escape: when cancer cells hijack the genes for chemotaxis and motility. *Annu Rev Cell Dev Biol*. 21: 695–718.
- DesMarais, V, Macaluso, F, Condeelis, J, and Bailly, M. (2004) Synergistic interaction between the Arp2/3 complex and cofilin drives stimulated lamellipod extension. *J Cell Sci*. 117: 3499-3510.
- Dong C-H, Kost B, Xia G, and Chua N-H (2001) Molecular identification and characterization of the *Arabidopsis* AtADF1, AtADF5 and AtADF6 genes. *Plant Mol Biol*. 45: 517-527.
- Dos Remedios, CG, Chhabra, D, Kekic, M, Dedova, IV, Tsubakihara, M, Berry, DA, and Nosworthy, NJ. (2003) Actin binding proteins: regulation of cytoskeletal microfilaments. *Physiol Rev*. 83: 433-473.
- El-Sibai, M, Nalbant, P, Pang, H, Flinn, RJ, Sarmiento, C, Macaluso, F, Cammer, M, Condeelis, JS, Hahn, KM, and Backer, JM. (2007) Cdc42 is required for EGF-stimulated protrusion and motility in MTLn3 carcinoma cells. *J Cell Sci*. 120: 3465-3474.
- Etienne-Manneville, S. (2004) Actin and microtubules in cell motility: which one is in control? *Traffic*. 5: 470-477.
- Fujibuchi, T, Abe, Y, Takeuchi, T, Imai, Y, Kamei, Y, Murase, R, Ueda, N, Shigemoto, K, Yamamoto, H, and Kito, K. (2005) Aip1/WDR1 supports mitotic cell rounding. *Biochem Biophys Res Comm*. 327: 268-275.
- Goldschmidt-Clermont, PJ, Machesky, LM, Doberstein, SK, and Pollard, TD. (1991) The mechanism of interaction of human platelet profiling with actin. *J Cell Biol* 113: 1081–1089.
- Goley, ED, and Welch, MD. (2006) The ARP2/3 complex: an actin nucleator comes of age. *Nat Rev Mol Cell Biol*. 7: 713–726.
- Hackett, AJ, Smith, HS, Springer, EL, Owens, RB, Nelson-Rees, WA, Riggs, JL, and Gardner, MB. (1977) Two syngenic cell lines from human breast tissue: the aneuploid mammary epithelial (Hs 578T) and the diploid myoepithelial (Hs 578Bst) cell lines. *J Natl Cancer Inst*. 58: 1795-1806.
- Hall, A. (2009) The cytoskeleton and cancer. *Cancer Metas Rev*. 28: 5-14.
- Hanahan, D, and Weinberg, RA. (2000) The hallmarks of cancer. *Cell*. 100: 57-70.



- Hill, TL, and Kirschner, MW. (1982) Subunit treadmilling of microtubules or actin in the presence of cellular barriers: possible conversion of chemical free energy into mechanical work. *Proc Natl Acad Sci USA*. 79: 490-494.
- Hopkins, AM, Pineda, AA, Winfree, ML, Brown, GT, Laukoetter, MG, and Nusrat, A. (2007) Organized migration of epithelial cells requires control of adhesion and protrusion through Rho kinase effectors. *Am J Physiol Gastrointest Liver Physiol*. 292: G806-G817.
- Hotulainen, P, Paunola, E, Vartiainen, MK, and Lappalainen, P. (2005) Actin-depolymerizing factor and cofilin-1 play overlapping roles in promoting rapid F-actin depolymerisation in mammalian nonmuscle cells. *Mol Biol Cell*. 16: 649-664.
- Hu, L, Zaloudek, C, Mills, GB, Gray, J, and Jaffe, RB. (2000) In vivo and in vitro ovarian carcinoma growth inhibition by a phosphatidylinositol 3-kinase inhibitor (LY294002). *Clin Cancer Res*. 6: 880-6.
- Iida, K, Moriyama, K, Matsumoto, S, Kawasaki, H, Nishida, E, and Yahara, I. (1993) Isolation of a yeast essential gene, COF1, that encodes a homologue of mammalian cofilin, a low-M(r) actin-binding and depolymerizing protein. *Gene*. 124: 115-120.
- Iida, K, and Yahara, I. (1999) Cooperation of two actin-binding proteins, cofilin and Aip1, in *Saccharomyces cerevisiae*. *Genes to Cells*. 4: 21-32.
- Kato, A, Kurita, S, Hyashi, A, Kaji, N, Ohashi, K, and Mizuno, K. (2008) Critical roles of actin-interacting protein 1 in cytokinesis and chemotactic migration of mammalian cells. *Biochem J*. 414(2): 261-270.
- Kile, BT, Panopoulos, AD, Stirzaker, RA, Hacking, DF, Tahtamouni, LH, Willson, TA, Mielke, LA, Henley, KJ, Zhang, JG, Wicks, IP, Stevenson, WS, Nurden, P, Watowich, SS, and Justice, MJ. (2007) Mutations in the cofilin partner Aip1/WDR1 cause autoinflammatory disease and macrothrombocytopenia. *Blood*. 110: 2371-2380.
- Kelly, T, Yan, Y, Osborne, RL, Athota, AB, Rozypal, TL, and Colclasure, JC. (1998) Proteolysis of extracellular matrix by invadopodia facilitates human breast cancer cell invasion and is mediated by matrix metalloproteinases. *Clin Exp Metastasis*. 16: 501-512.
- Konzok, A, Weber, I, Simmeth, E, Hacker, U, Maniak, M, and Muller-Taubenberger, A. (1999) DAip1, a *Dictyostelium* homologue of yeast actin-interacting protein 1, is involved in endocytosis, cytokinesis, and motility. *J Cell Biol*. 146(2): 453-464.

- Kueh, HY, Charras, GT, Mitchison, TJ, and Brieher, WM. (2008) Actin disassembly by cofilin, coronin, and Aip1 occurs in bursts and is inhibited by barbed-end cappers. *J Cell Biol.* 182(2): 341-353.
- Landolph, JR, Verma, A, Ramnath, J, and Clemens, F. (2002) Molecular biology of deregulated gene expression in transformed C3H/10T1/2 mouse embryo cell lines induced by specific insoluble carcinogenic nickel compounds. *Envir Health Perspec.* 110(5): 845-850.
- Lappalainen, P, Kessels, MM, Cope, MJ, and Drubin, DG. (1998) The ADF homology (ADF-H) domain: a highly exploited actin-binding module. *Mol Biol Cell.* 9: 1951-1959.
- Le Clainche, C, and Carlier, MF. (2008) Regulation and actin assembly associated with protrusion and adhesion in cell migration. *Physiol Rev.* 88: 489-513.
- Lenke, LE, Paine-Murrieta, GD, Taylor, CW, and Powis, G. (1999) Wortmannin inhibits the growth of mammary tumors despite the existence of a novel wortmannin-insensitive phosphatidylinositol-3-kinase. *Cancer Chemother Pharmacol.* 44: 491-7.
- Leyman, S, Sidani, M, Ritsma, L, Waterschoot, D, Eddy, R, Dewitte, D, Debeir, O, Decaestecker, C, Vanderkerckhove, J, van Rheenen, J, Ampe, C, Condeelis, J, and van Troys, M. (2009) Unbalancing the PI(4,5)P2-cofilin interaction impairs cell steering. *Mol Biol Cell.*
- Li, J, Brieher, WM, Scimone, ML, Kang, SJ, Zhu, H, Yin, H, von Andrian, UH, Mitchison, T, and Yuan, J. (2007) Caspase-11 regulates cell migration by promoting Aip1-cofilin-mediated actin depolymerisation. *Nat Cell Biol.* 1-20.
- Li, D, and Roberts, R. (2001) WD-repeat proteins: structure characteristics, biological function, and their involvement in human disease. *Cell Mol Life Sci.* 58: 2085-2097.
- Linder, S, and Kopp, P. (2005) Podosomes at a glance. *J Cell Sci.* 118: 2079-2082.
- Lomax, MI, Gong, TL, Cho, Y, Huang, L, Oh, SH, Adler, HJ, Raphael, Y, and Altschuler, RA. (2001) Differential gene expression following noise trauma in birds and mammals. *Noise Health.* 3(11): 19-35.
- Lundquist, EA. (2009) The finer points of filopodia. *PLoS Biol.* 7(6): e1000142.
- Ma, YY, Wei, SJ, Lin, YC, Lung, JC, Chang, TC, and Whang-Peng, J. (2000) PIK3CA as an oncogene in cervical cancer. *Oncogene.* 19: 2739-44.
- Machesky, LM, Reeves, E, Wientjes, F, Mattheyse, FJ, Grogan, A, Totty, NF, Burlingame, AL, Hsuan, JJ, and Segal, AW. (1997) Mammalian actin-related

- protein 2/3 complex localizes to regions of lamellipodial protrusions and is composed of evolutionarily conserved proteins. *Biochem J.* 15(328): 105-112.
- Machesky, LM. (2008) Lamellipodia and filopodia in metastasis and invasion. *FEBS Letters.* 582: 2102-2111.
- Maciver, SK, and Hussey, PJ. (2002) The ADF/cofilin family: actin-remodeling proteins. *Genome Biol.* 3(5): 3007.1-3007.12.
- Mohri, K, and Ono, S. (2003) Actin filament disassembling activity of *Caenorhabditis elegans* actin-interacting protein 1 (UNC-78) is dependent on filament binding by a specific ADF/cofilin isoform. *J Cell Sci.* 116: 4107-4118.
- Mohri, K, Vorobiev, S, Fedorov, AA, Almo, SC, and Ono, S. (2004) Identification of functional residues on *Caenorhabditis elegans* actin-interacting protein 1 (UNC-78) for disassembly of actin depolymerising factor/cofilin-bound actin filaments. *J Biol Chem.* 279(30): 31697-31707.
- Mohri, K, Ono, K, Yu, R, Yamashiro, S, and Ono, S. (2006) Enhancement of actin-depolymerizing factor/cofilin-dependent actin disassembly by actin-interacting protein 1 is required for organized actin filament assembly in the *Caenorhabditis elegans* body wall muscle. *Mol Biol Cell.* 17: 2190-2199.
- Moon, A, and Drubin, DG. (1995) The ADF/cofilin proteins: stimulus-responsive modulators of actin dynamics. *Mol Biol Cell.* 6: 1423-1431.
- Moon, AL, Janmey, PA, Louie, KA, and Drubin, DG. (1993) Cofilin is an essential component of the yeast cortical cytoskeleton. *J Cell Biol.* 120: 421-435.
- Morgan, TE, Lockerbie, RO, Minamide, LS, Browning, MD, and Bamburg, JR. (1993) Isolation and characterization of a regulated form of actin-depolymerizing factor. *J Cell Biol.* 122; 623-633.
- Nakashima, K, Sato, N, Nakagaki, T, Abe, H, Ono, S, and Obinata, T. (2005) Two mouse cofilin isoforms, muscle-type (MCF) and non-muscle type (NMCF), interact with F-actin with different efficiencies. *J Biochem.* 138: 519-526.
- Nishida, E, Maekawa, S, and Sakai, H. (1984) Cofilin, a protein in porcine brain that binds to actin filaments and inhibits their interactions with myosin and tropomyosin. *Biochem.* 23: 5307-5313.
- Nishida, E, Iida, K, Yonezawa, N, Koyasu, S, Yahara, I, and Sakai, H. (1987) Cofilin is a component of intranuclear and cytoplasmic actin rods induced in cultured cells. *Proc Natl Acad Sci USA.* 84: 5262-5266.

- Nishita, M, Tomizawa, C, Yamamoto, M, Horita, Y, Ohasi, K, and Mizuno, K. (2005) Spatial and temporal regulation of cofilin activity by LIM kinase and slingshot is critical for directional cell migration. *J Cell Biol.* 171(2): 349-359.
- Noone, TE, and Hubberstey, AV. (2004) Human WDR1 interacts with actin and is involved in cell attachment and cytoskeletal rearrangement. *Unpublished.*
- Ohashi, K, Nagata, K, Maekawa, M, Ishizaki, T, Narumiya, S, and Mizuno, K. (2000) Rho-associated kinase ROCK activates LIM-kinase 1 by phosphorylation at threonine 508 within the activation loop. *J Biol Chem.* 275: 3577–3582
- Okada, K, Blanchoin, L, Abe, H, Chen, H, Pollard, TD, and Bamburg, JR. (2002) *Xenopus* actin interacting protein 1 (XAip1) enhances cofilin fragmentation of filaments by capping filament ends. *J Biol Chem.* 277: 43011–43016.
- Okada, K, Obinata, T, and Abe, H. (1999) XAIP1: a *Xenopus* homologue of yeast actin interacting protein 1 (AIP1), which induces disassembly of actin filaments cooperatively with ADF/cofilin family proteins. *J Cell Sci.* 112: 1553-1565.
- Okada, K, Ravi, H, Smith, EM, and Goode, BL. (2006) Aip1 and cofilin promote rapid turnover of yeast actin patches and cables: a coordinated mechanism for severing and capping filaments. *Mol Biol Cell.* 17: 2855-2868.
- Olson, MF, and Sahai, E. (2008) The actin cytoskeleton in cancer cell motility. *Clin Exp Metas.*
- Ono, S. (2001) The *Caenorhabditis elegans unc-78* gene encodes a homologue of actin interacting protein 1 required for organized assembly of muscle actin filaments. *J. Cell Biol.* 152: 1313–1320
- Ono, S. (2003) Regulation of actin filament dynamics by actin depolymerizing factor/cofilin and actin-interacting protein 1: new blades for twisted filaments. *Biochem.* 42(46): 13363-13370.
- Ono S, and Benian GM. (1998) Two *Caenorhabditis elegans* actin depolymerizing factor/cofilin proteins, encoded by the *unc-60* gene, differentially regulate actin filament dynamics. *J Biol Chem.* 273: 3778-3783.
- Ono, S, Minami, N, Abe, H, and Obinata, T. (1994) Characterization of a novel cofilin isoform that is predominantly expressed in mammalian skeletal muscle. *J Biol Chem.* 269: 15280–15286.
- Ono, S, Mohri, K, and Ono, K. (2004) Microscopic evidence that actin-interacting protein 1 actively disassembles actin-depolymerizing factor/cofilin-bound actin filaments. *J Biol Chem.* 279(14): 14207-14212.

- Oshima, RG. (2007) Intermediate filaments: a historical perspective. *Exp Cell Res.* 313(10): 1981-1994.
- Pellegrin, S, and Mellor, H. (2007) Actin stress fibres. *J Cell Sci.* 120: 3491-3499.
- Prag, S, and Adams, JC. (2003) Molecular phylogeny of the kelch-repeat superfamily reveals an expansion of BTB/kelch proteins in animals. *BMC Bioinform.* 4(42).
- Pring, M, Evangelista, M, Boone, C, Yang, C, and Zigmond, SH. (2003) Mechanism of formin-induced nucleation of actin filaments. *Biochem.* 42: 486-496.
- Ren, N, Charlton, J, and Adler, PN. (2007) The *flare* gene, which encodes the Aip1 protein of *Drosophila*, functions to regulate F-actin disassembly in pupal epidermal cells. *Genetics.* 176: 2223-2234.
- Roberts, SG. (2000) Mechanisms of action of transcription activation and repression domains. *Cell Mol Life Sci.* 57: 1149-1160.
- Rodal, AA, Tetreault, JW, Lappalainen, P, Drubin, DG, and Amberg, DC. (1999) Aip1p interacts with cofilin to disassemble actin filaments. *J Cell Biol.* 145(6): 1251-1264.
- Rogers, SL, Wiedemann, U, Stuurman, N, and Vale, RD. (2003) Molecular requirements for actin-based lamella formation in *Drosophila* S2 cells. *J Cell Biol.* 162(6): 1079-1088.
- Samstag, Y, Eibert, SM, Klemke, M, and Wabnitz, GH. (2003) Actin cytoskeletal dynamics in T lymphocyte activation and migration. *J Leuk Biol.* 73: 30-48.
- Scott, RW, and Olson, MF. (2007) LIM kinases: function, regulation and association with human disease. *J Mol Med.* 85: 555-568.
- Sept, D, Xu, J, Pollard, TD, and McCammon, JA. (1999) Annealing accounts for the length of actin filaments formed by spontaneous polymerization. *Biophys J.* 77: 2911-2919.
- Shayesteh, L, Lu, Y, Kuo, WL, Baldocchi, R, Godfrey, T, and Collins, C. (1999) PIK3CA is implicated as an oncogene in ovarian cancer. *Nat Genet.* 21: 99-102.
- Sheterline, P, Clayton, J, and Sparrow, J. (1995) Actin. *Protein Profile.* 2: 1-103.
- Shin, DH, Lee, E, Chung, YH, Mun, GH, Park, JY, Lomax, MI, and Oh, SH. (2004) Subcellular localization of WD40 repeat 1 protein in PC12 rat pheochromocytoma cells. *Neurosci Letters.* 367: 399-409.
- Sidani, M, Wessels, D, Mouneimne, G, Ghosh, M, Goswami, S, Sarmiento, C, Wang, W, Kuhl, S, El-Sibai, M, Backer, JM, Eddy, R, Soll, D, and Condeelis, J. (2007)

- Cofilin determines the migration behaviour and turning frequency of metastasis cancer cells. *J Cell Biol.* 179(4):777-791.
- Smith, HS. (1979) In vitro properties of epithelial cell lines established from human carcinomas and nonmalignant tissue. *J Natl Cancer Inst.* 62: 225-230.
- Smith, TF, Gaitatzes, C, Saxena, K, and Neer, EJ. (1999) The WD repeat: a common architecture for diverse functions. *Trends Biochem. Sci.* 24: 181-185.
- Song, X, Chen, X, Yamaguchi, H, Mouneimne, G, Condeelis, JS, and Eddy, RJ. (2006) Initiation of cofilin activity in response to EGF is uncoupled from cofilin phosphorylation and dephosphorylation in carcinoma cells. *J Cell Sci.* 119: 2871-2881.
- Soule, HD, Vazquez, J, Long, A, Albert, S, and Brennan, M. (1973) A human cell line from a pleural effusion derived from a breast carcinoma. *J Natl Cancer Inst.* 51: 1409-1416.
- Stylli, SS, Kaye, AH, and Lock, P. (2008) Invadopodia: at the cutting edge of tumour invasion. *J Clin Neurosci.* 15: 725-737.
- Suyama, E, Wadhwa, R, Kawasaki, H, Yaguchi, T, Kaul, SC, Nakajima, M, and Taira, K. (2004) LIM-kinase-2 targeting as a possible anti-metastasis therapy. *J Gene Med.* 6: 357-363.
- Svitkina, TM, and Borisy, GG (1999) Arp2/3 complex and actin depolymerizing factor/cofilin in dendritic organization and treadmilling of actin filament array in lamellipodia. *J Cell Biol.* 145: 1009-1026.
- Theriot, JA. (1997) Accelerating on a treadmill: ADF/cofilin promotes rapid actin filament turnover in the dynamic cytoskeleton. *J Cell Biol.* 136(6): 1165-1168.
- Tsuji, T, Miyoshi, T, Higashida, C, Narumiya, S, and Watanabe, N. (2009) An order of magnitude faster Aip1-associated actin disruption than nucleation by the Arp2/3 complex in lamellipodia. *PLOS.* 4(3): 1-13.
- van Dijk, MA, Floore, AN, Kloppenborg, KI, and van 't Veer, LJ. (1997) A functional assay in yeas for the human estrogen receptor displays wild-type and variant estrogen receptor messenger RNAs present in breast carcinoma. *Cancer Res.* 57: 3478-3485.
- Van Rheenem, J, Song, X, van Roosmalen, W, Cammer, M, Chen, X, DesMarais, V, Yip, S, Backer, JM, Eddy, RJ, and Condeelis, JS. (2007) EGF-induced PIP<sub>2</sub> hydrolysis releases and activates cofilin locally in carcinoma cells. *J Cell Biol.* 179(6): 1247-1259.

- Van Troys, M, Huyck, L, Leyman, S, Dhaese, S, Vandekerckhove, J, and Ampe, C. (2008) Ins and outs of ADF/cofilin activity and regulation. *Eur J Cell Biol.* 1-19.
- Voegtli, WC, Madrona, AY, and Wilson, DK. (2003) The structure of Aip1p, a WD repeat protein that regulates cofilin-mediated actin depolymerisation. *J Biol Chem.* 278(36): 34373-34379.
- Wang, YL. (1985) Exchange of actin subunits at the leading edge of living fibroblasts: possible role of treadmilling. *J Cell Biol.* 101: 597-602.
- Wang, W, Mouneimne, G, Sidani, M, Wyckoff, J, Chen, X, Makris, A, Goswami, S, Bresnick, AR, and Condeelis, JS. (2006) The activity status of cofilin is directly related to invasion, intravasation, and metastasis of mammary tumors. *J Cell Biol.* 173(3): 395-404.
- Wegner, A. (1976) Head to tail polymerization of actin. *J Mol Biol.* 108: 139–150.
- Welch, MD, Iwamatsu A, and Michison TJ. (1997) Actin polymerization is induced by Arp2/3 protein complex at the surface of *Listeria monocytogenes*. *Nature* 385: 265–269.
- Yamaguchi, H, and Condeelis, J. (2006) Regulation of the actin cytoskeleton in cancer cell migration and invasion. *BBA.* 4C(2): 1-11.
- Yamaguchi, H, Pixley, F, and Condeelis, J. (2006) Invadopodia and podosomes in tumor invasion. *Eur J Cell Biol.* 85: 213-218.
- Yamaguchi, H, Lorenz, M, Kempiak, S, Sarmiento, C, Coniglio, S, Symons, M, Segall, J, Eddy, R, Miki, H, and Takenawa, T. (2005) Molecular mechanisms of invadopodium formation: the role of the N-WASPArp2/3 complex pathway and cofilin. *J Cell Biol.* 168(3): 441–52.
- Yamamoto, T, Poon, D, Weil, PA, and Horikoshi, M. (1997) Molecular genetic elucidation of the tripartite structure of the *Schizosaccharomyces pombe* 72kDa TF11D subunit which contains a WD40 structural motif. *Genes Cells.* 2(4): 245-254.
- Yamashiro, S, Cox, EA, Baillie, DL, Hardin, JD, and Ono, S. (2008) Sarcomeric actin organization is synergistically promoted by tropomodulin, ADF/cofilin, Aip1, and profiling in *C. elegans*. *J Cell Sci.* 121(23): 3867-3877.
- Yamazaki, D, Kurisu, S, and Takenawa, T. (2005) Regulation of cancer cell motility through actin reorganization. *Cancer Sci.* 96(7): 379-386.
- Yilmaz, M, and Christofori, G. (2009) EMT, the cytoskeleton, and cancer cell invasion. *Cancer Metas Rev.* 28: 15-33.

Yonezawa, N, Nishida, E, Iida K, Yahara, I, and Sakai, H. (1990) Inhibition of the interactions of cofilin, destrin, and deoxyribonuclease I with actin by phosphoinositides. *J Biol Chem.* 265: 8382–8386.

Yoshioka, K, Foletta, V, Bernard, O, and Itoh, K. (2003) A role for LIM-kinase in cancer invasion. *Proc Natl Acad Sci.* 100: 7247–7252.

Zebda, N, Bernard, O, Bailly, M, Welte, S, Lawrence, DS, and Condeelis, JS. (2000) Phosphorylation of ADF/cofilin abolishes EGF-induced actin nucleation at the leading edge and subsequent lamellipod extension. *J. Cell Biol.* 151: 1119–1127.

## Appendix A

### List of antibodies and their specifications

Primary	Solution	Ratio	Company
anti-Cofilin	TTBS	1:1000	Cytoskeleton, Inc.
anti-GAPDH	TTBS	1:1000	Santa Cruz Biotechnology
anti-GFP	TTBS	1:5000	Rockland, Inc.
anti-HA	TTBS	1:10000	n/a
anti-phospho-cofilin	Dilution buffer	1:1000	Cell Signalling Technology
anti-actin	TTBS	1:1000	Chemicon International

Secondary	Solution	Ratio	Company
goat anti-rabbit	TTBS	1:4000	Invitrogen
goat anti-mouse	TTBS	1:4000	Invitrogen
goat anti-rabbit	TTBS	1:5000	Invitrogen
goat anti-mouse	TTBS	1:4000	Invitrogen
goat anti-rabbit	Blocking solution	1:2000	Invitrogen
goat anti-mouse	TTBS	1:4000	Invitrogen



## **Vita Auctoris**

NAME: Jessica Kathleen Cucullo

YEAR OF BIRTH: 1985

PLACE OF BIRTH: Sault Ste. Marie, ON

EDUCATION: University of Windsor, Windsor, ON  
M.Sc. Biological Sciences  
2007-2009

University of Western Ontario, London, ON  
B.Sc. Honours Biology  
2003-2007

St. Basil's Secondary School, Sault Ste. Marie, ON  
1999-2003